



Strålsäkerhetsmyndigheten

Swedish Radiation Safety Authority

Author: Lars Olof Jernkvist
Quantum Technologies AB, Uppsala Science Park

Research

2020:02

Models for axial gas flow
and mixing in LWR fuel rods

SSM perspective

Background

Fission gases inside a fuel rod plays an important role in the behaviour of the fuel, both during normal operation and during events and accidents. Fission gases are released from inside the fuel pellets to the gap between the pellet and the cladding tube and then flow to the plenum volume at the top of the fuel rod. In high burnup fuel, this axial flow to the plenum volume can be blocked because of pellet-cladding gap closure.

The presence of fission gases in the pellet-cladding gap is important for the rod internal pressure and for the pellet-cladding heat transfer. While these effects are considered in most computer codes for fuel rod thermal-mechanical analyses, the axial flow of fission gases is generally not. This flow can be important for several reasons, for example for removal of fission gases from the active region during normal operation, in the complex behaviour during load-follow operation and for how the fission gases propagates during an event.

Results

The results include the development, implementation and verification of models for axial gas transport and gas mixing in the pellet-cladding gap. The models take into account gas transport both by axial pressure gradients and by diffusion, and they are intended for use in the FRAPCON and FRAPTRAN codes for further analysis of fuel behaviour. Calculations that verify the correctness of the numerical implementation and validation against a few experiments have been done.

Relevance

With this project, SSM has obtained a computer code that can model axial fission gas transport in a fuel rod. SSM has also gained insight into how such a model is implemented in a computer code, with what assumptions and limitations. This is of great importance when reviewing safety analyses for nuclear fuel. Furthermore, this project is part of the international development work and enables active participation in international contexts.

Need for further research

The development and implementation of models for analysing axial gas flow and fission gas mixing needs to be complemented with validation against more complex tests on fuel with higher burnup. This validation will also reveal the need for further development. On a longer time scale, much research and development remains to fully understand the behaviour of high burnup fuel.

Project information

Contact person SSM: Anna Alvestav

Reference: SSM2018-4296 / 7030270-00



Strål
säkerhets
myndigheten

Swedish Radiation Safety Authority

Author: Lars Olof Jernkvist
Quantum Technologies AB, Uppsala Science Park

2020:02

Models for axial gas flow and mixing in LWR fuel rods

Date: March 2020

Report number: 2020:02 ISSN: 2000-0456

Available at www.stralsakerhetsmyndigheten.se

This report concerns a study which has been conducted for the Swedish Radiation Safety Authority, SSM. The conclusions and viewpoints presented in the report are those of the author/authors and do not necessarily coincide with those of the SSM.

Models for axial gas flow and mixing in LWR fuel rods

Report TR19-002v1, December 9, 2019

Lars Olof Jernkvist

Quantum Technologies AB
Uppsala Science Park
SE-75183 Uppsala, Sweden



Summary

The thermal-mechanical behavior of light water reactor fuel rods may, under certain conditions, be affected by axial transport of gas that reside in the pellet-cladding gap and other internal volumes of the rods. The conditions of interest range from mild overpower transients to reactor accident scenarios, such as loss-of-coolant or reactivity-initiated accidents.

This report presents a computational model for axial transport and mixing of the free gas inventory in light water reactor fuel rods. The model is designed for analyses of a wide spectrum of operating conditions for the fuel, ranging from normal reactor operation to severe accident scenarios, and it is intended to be introduced into the FRAPCON and FRAPTRAN fuel rod analyses programs. In the report, the model is developed from governing equations for the involved phenomena, numerically implemented in a set of FORTRAN subroutines, and validated against analytical solutions as well as selected gas flow experiments.

The model calculates multicomponent gas flow due to axial pressure gradients as well as diffusion along the pellet-cladding gap. The gas flow is calculated as a function of space and time, based on fuel rod deformations, fission gas release and temperature changes of the fuel rod gas inventory. In addition, outleakage of gas through a postulated cladding breach can be modelled at an arbitrary axial position of the fuel rod.

The equations for conservation of mass and momentum for the gas, combined with the Stefan-Maxwell equations for multicomponent diffusion, are discretized in space by use of a quasi one-dimensional finite volume model of the pellet-cladding gap and other internal volumes of the fuel rod. The resulting interconnected systems of equations are solved with respect to time by use of an efficient, implicit, time stepping scheme, in which the Newton-Raphson method is used for internal iterations.

The correctness of the numerical implementation of the model is verified by comparing calculated results with analytical solutions of simple problems. The model is also successfully validated against a limited number of selected experiments.

Sammanfattning

Det termomekaniska beteendet hos bränslestavar till lättvattenreaktorer kan, under vissa förhållanden, påverkas av axiell transport av den gas som finns i stavarnas kuts-kapslingsgap och andra inre hålrum. Detta gäller alltifrån milda övereffektransienter till haverisituationer i reaktorn, såsom olyckor med kylmedelsförlust eller snabba reaktivitetstillskott.

Föreliggande rapport presenterar en beräkningsmodell för axiell transport och blandning av det fria gasinnehållet i bränslestavar till lättvattenreaktorer. Modellen är utformad för analyser av vitt skilda driftförhållanden för bränslet, från normal reaktordrift till svåra olyckor, och den är avsedd att inlemmas i bränsleanalysprogrammen FRAPCON och FRAPTRAN. I rapporten utvecklas modellen med utgångspunkt från de ekvationer som beskriver inblandade fenomen, den implementeras numeriskt i en uppsättning beräkningsrutiner skrivna i programmeringsspråket FORTRAN, och dess giltighet bekräftas genom jämförelser med analytiska lösningar och utvalda gasflödesexperiment.

Modellen beräknar flerkomponentflödet av gas på grund av axiella tryckgradienter och diffusion längs med kuts-kapslingsgapet. Gasflödet beräknas med avseende på tid och rum, baserat på bränslestavens deformation, fissionsgasfrigörelse och gasinnehållets temperaturförändringar. Dessutom kan utläckage av gas genom en postulerad kapslingsskada modelleras vid en godtycklig axiell position längs staven.

Konserveringslagarna för gasens massa och rörelsemängd, i kombination med Stefan-Maxwells ekvationer för flerkomponentsdiffusion, diskretiseras rumsligt med en kvasi-endimensionell finit volymmodell av kuts-kapslingsgapet och andra inre hålrum hos bränslestaven. Det resulterande systemet av kopplade ekvationer löses med avseende på tid med hjälp av en effektiv, implicit, tidsstegningsmetod, i vilken Newton-Raphsons metod används för interna iterationer.

Genom jämförelse av beräkningsresultat med analytiska lösningar till enkla problem bekräftas att modellens numeriska implementering är korrekt. Modellen utvärderas även framgångsrikt genom jämförelse med ett begränsat antal utvalda experiment.

Contents

Summary	I
Sammanfattning	II
1 Introduction	1
1.1 Background and historical perspective	1
1.2 Phenomena of importance to fuel rod behaviour	2
1.3 Scope and organization of the report	4
2 The FRAPCON/FRAPTRAN computational framework	5
2.1 Spatial discretization of the fuel rod	5
2.1.1 Axial segmentation	5
2.1.2 Gas volumes within each axial segment	6
2.2 Properties of fuel rod gas inventory	7
2.2.1 Gas composition	7
2.2.2 Gas temperature and pressure distribution	7
2.2.3 Properties of the flowing gas	8
3 Governing equations for gas flow and mixing	9
3.1 Basic assumptions and notation	9
3.2 Equation of state for the gas	10
3.3 Equation for conservation of mass	10
3.3.1 Bulk flow of gas	11
3.3.2 Flow of individual gas species	12
3.4 Equation for conservation of momentum	12
3.4.1 Bulk flow of gas	12
3.4.2 Flow resistance from wall friction	13
3.5 Multicomponent diffusion	14
3.5.1 General equations	15
3.5.2 Stefan-Maxwell equations	15
3.5.3 Simplified equations	16
3.6 Outleakage of gas through a cladding breach	17
4 Numerical solution of the gas flow equations	19
4.1 Determination of bulk molar flow	19
4.1.1 Spatial discretization of the conservation equations	19
4.1.2 Temporal discretization of the conservation equations	22
4.1.3 Fully discretized conservation equations	22
4.1.4 Application of Newton-Raphson iterations	23
4.2 Redistribution of gas constituents	24
4.3 Criterion on convergence in iterations	25
5 The GASMIX set of subroutines	27
5.1 Flowchart of the GASMIX subroutine	28
5.2 User-defined input to GASMIX	28
6 Model verification and validation	31
6.1 Gas mixing by diffusion	31

6.1.1	Analytical reference case	31
6.1.2	Computational modelling	32
6.1.3	Results	33
6.2	Gas flow due to pressure gradients	34
6.2.1	The INEL gas flow experiments	34
6.2.2	Computational modelling	35
6.2.3	Results	36
7	Conclusions and outlook	39
	References	43
A	Properties of the flow channel geometry	47
A.1	Flow channel Hagen number	47
A.2	Flow channel cross-sectional area	48
B	Calculation of binary diffusion coefficients	51
C	Explicit expressions for discretized equations	55
C.1	Bulk flow of gas	55
C.2	Flow of gas constituents	56
D	GASMIX source code structure	59
D.1	Subroutines used in the GASMIX algorithm	59
D.2	Data structures used in GASMIX	62
D.2.1	Flow channel data	62
D.2.2	Gas inventory data	63
D.2.3	Gas thermodynamic data	63
D.2.4	Gas transport data	64
D.2.5	Work arrays for equation solvers	64

1 Introduction

1.1 Background and historical perspective

Axial transport and mixing of gas that resides in the pellet-cladding gap and other internal volumes of light water reactor (LWR) fuel rods are important to the thermal-mechanical behaviour of the fuel rods. For example, gaseous fission products with low thermal conductivity, notably xenon and krypton, which are released from the fuel pellets during operation, deteriorate the thermal conductance of the pellet-cladding gap. The increase in fuel temperature that results from this thermal insulation of the fuel will then, in turn, enhance further fission gas release. This undesired spiral of increasing fission gas release and increasing fuel temperature is eventually broken when the released fission gases mix with the high-conductivity helium that is used as a fill gas in LWR fuel rods. However, most of the fission gases are released in the hot central part of the fuel rod, whereas the helium fill gas is located in gas plena at one or both ends of the fuel rod. The long and narrow flow channel that connects these regions delays axial transport and mixing of gases.

Mixing of fission gases with the fuel rod helium fill gas is therefore a rather slow phenomenon, the time dependence of which is necessary to take into account in order to correctly determine the thermal conductance of the pellet-cladding gap and the fuel temperature. This is particularly important when analysing the fuel behaviour under overpower transients or load-follow operation. In the 1980s, axial gas mixing in LWR fuel rods was extensively studied in a series of in-reactor experiments that were carried out in the Halden reactor, Norway [1, 2, 3, 4]. In Halden, out-of-reactor experiments on gas mixing were also conducted on an electrically heated fuel rod simulator [5]. At the same time, computational models for axial gas transport and mixing were developed, with the aim to implement them in various fuel rod analysis programs [6, 7, 8]. It seems that these efforts were in vain, since most computer programs used for fuel rod thermal-mechanical analyses today do *not* model axial gas mixing [9].

Axial gas transport within a fuel rod may also be important to the fuel rod behavior in accident conditions, such as loss-of-coolant accidents (LOCAs). In a design basis LOCA, a brittle fracture of the primary reactor coolant pipe is assumed to occur, resulting in a sudden loss of coolant and a drop of coolant pressure. The loss of coolant causes a rapid fuel rod temperature rise, resulting in decreased cladding strength and a significant rod internal overpressure. This combination may cause local distension, known as "ballooning" of the weakened cladding at axial positions with particularly high temperature.

Axial gas flow can prevent or assist cladding ballooning in a LOCA, depending on whether extensive transient fission gas release occurs during the acci-

dent and at what time during the accident the ballooning occurs. If ballooning occurs early in the LOCA and transient fission gas release is limited, axial gas flow from the fuel rod plena to the ballooning region will assist the ballooning by providing gas that drives the local deformation. On the other hand, if extensive transient fission gas release occurs, which is typically the case for very high burnup fuel, axial gas flow may prevent the ballooning by reducing the otherwise high gas pressure that would arise locally in the overheated part of the fuel rod where the transient gas release occurs.

Ballooning may also occur later in the LOCA, during the re-flood phase. In this phase of the accident, the emergency core cooling systems re-flood the core with water that flows upward through the core, cooling the lower portion of the fuel rods first. In this case, axial gas flow from the overheated part of the fuel rod to the effectively cooled lower portion of the rod will help prevent ballooning of the cladding.

The importance of axial gas flow to the ballooning and rupture of LWR fuel rods under LOCA was recognized early, and in the mid-1970s, axial gas flow experiments were conducted in the USA on six full-length fuel rods that had been irradiated to a rod average burnup around $25 \text{ MWd}(\text{kgU})^{-1}$ in a commercial pressurized water reactor (PWR) [10]. One of the rods was extensively characterized by use of metallography and ceramography, with the aim to quantitatively determine the axial flow path for the gas. Some of these experiments are further described and used for model validation in section 6.2 of this report. More recently, in-reactor LOCA simulation tests on LWR fuel rods have shown that axial gas flow may be very slow in fuel rods with higher burnup than those in the aforementioned experiments from the 1970s [11, 12, 13]. The reason is that the pellet-cladding gap, which makes up most of the axial flow channel for the gas, is virtually closed in high burnup fuel rods, at least as long as the cladding distension is limited. The implications of the restricted axial gas flow in some of these experiments have been studied by use of computational models [14].

1.2 Phenomena of importance to fuel rod behaviour

From the studies mentioned in the foregoing section, we conclude that two different phenomena related to axial gas flow and mixing have potential to affect the thermal-mechanical behaviour of LWR fuel rods under various operating conditions:

- Bulk flow of gas, caused by axial pressure gradients.
- Mixing of gas under uniform pressure, caused by diffusion.

The first phenomenon is important mostly for off-normal and accident con-

ditions, where it has the potential to affect the cladding rupture behaviour. In addition to LOCAs, the phenomenon is relevant also for some scenarios of reactivity-initiated accidents (RIAs) that involve significant overheating of the cladding tube [15]. Axial pressure gradients may arise inside the fuel rod due to fission gas release, temperature changes of the gas, and deformation of the fuel pellets and/or the cladding tube. Bulk flow of gas induced by pressure gradients is comparatively fast, generally leading to equilibrium conditions within a few minutes. However, the time needed for this pressure equilibration is strongly dependent on the cross-sectional area that is open for gas flow within the fuel rod. In high-burnup fuel, the pellet and cladding is in contact. Unless the pellets are annular, the gas flow is then confined to pellet cracks and the small annular clearance that may remain between the pellet and cladding due to the surface roughnesses of the two objects. The flow path made up of pellet cracks is extremely tortuous [10].

The axial bulk flow will generally lead to removal of fission gas from the peak power section of the fuel rod during an increase in power, but it will not contribute to the dilution of fission gases in the peak power area until the power is lowered and the bulk flow changes its direction. This mechanism of gas mixing under power fluctuations is generally referred to as the "pumping effect". It may be important under LWR load-follow operation, since the frequent changes of rod power will induce bulk transport of gas between the active (fuelled) part of the rod and gas plena. The direction of the bulk flow changes as the rod power is increased or decreased, and the bidirectional gas transport effectively contributes to mixing of gas constituents.

The second phenomenon is important for normal steady-state operation and mild overpower transients, since it has the potential to affect the thermal conductance of the pellet-cladding gap, and hence, the fuel temperature. The gas mixing takes place under virtually uniform pressure conditions, i.e. in the absence of pressure gradients. Consequently, there is no net transport of mass inside the fuel rod, but if there are concentration gradients among individual gas species in the gas, there will be equilibrating flows of these gas components due to diffusion. Diffusive mixing is a much slower phenomena than bulk flow under pressure gradients. The time scale for concentration equilibration by diffusion is in the order of hours or days. At a rapid increase in power, the released fission gases may therefore quickly fill the pellet-cladding gap through pressure equilibrating bulk flow, and then remain nearly unaffected in the gap for several hours after the power excursion. The resulting thermal insulation of the fuel may then lead to further release of fission gas.

Since the two phenomena are relevant for different operating conditions of the fuel, computational models have usually been developed for either of the phenomena - the author is unaware of computational models that treat both phenomena in combination. However, in this report, a general model is proposed, in which bulk flow of gas and diffusive mixing are treated in combi-

nation. The proposed model is applicable to both normal steady-state fuel operation and accident conditions. It is particularly suited for modelling the behaviour of LWR fuel under load-follow operation, where the two phenomena are believed to interact.

1.3 Scope and organization of the report

The models for axial gas flow and mixing presented in this report are intended for implementation in the FRAPCON and FRAPTRAN computer programs. These programs are developed and maintained by the Pacific Northwest National Laboratory (PNNL) for the United States Nuclear Regulatory Commission (US NRC), and they are used worldwide for thermal-mechanical analyses of LWR fuel rods under steady-state operation and transient conditions, respectively. The same set of models is foreseen to be implemented in both programs, which are henceforth referred to as the "host codes" for the presented models.

The design of the presented gas flow and mixing models is affected by the structure and scope of the host codes. For example, the presented models depend on the host codes for generating necessary boundary conditions in terms of the space-time variation of fission gas release and gas temperatures in various partial volumes of the modelled fuel rod. Consequently, we start in section 2 by defining the computational framework provided by FRAPCON and FRAPTRAN. Emphasis is placed on the spatial and temporal discretization applied in these host codes, and how the volume, temperature and composition of the rod internal gas inventory are calculated. The governing equations for axial gas flow and mixing to be solved in this computational framework are then presented in section 3, and the numerical methods applied for solving them are presented in section 4. The solution methods have been numerically implemented in a set of FORTRAN subroutines and functions, intended for incorporation in FRAPCON and FRAPTRAN. The structure of this source code is described in section 5. In section 6, the implemented models are validated against analytical solutions for binary diffusion and the aforementioned experiments on axial gas flow in irradiated PWR fuel rods. Conclusions of the work are finally given in section 7, where also some suggestions for further work are given.

2 The FRAPCON/FRAPTRAN computational framework

The models presented in this report are intended for implementation in the US NRC FRAPCON and FRAPTRAN fuel performance analysis programs [16, 17]. These are sibling programs with similar structure, where FRAPTRAN is designed specifically for analysing the fuel rod thermal-mechanical behaviour in LWR transient and accident conditions. Since FRAPTRAN lacks models for long-term steady-state fuel operation, it requires that burnup-dependent pre-accident fuel rod conditions are defined as input. This input is usually generated by use of FRAPCON, which, in contrast to FRAPTRAN, is designed for fuel rod thermal-mechanical analyses of normal, steady-state fuel operation. If the programs are used together, the burnup-dependent data needed as input by FRAPTRAN are transferred from FRAPCON via an interface.

2.1 Spatial discretization of the fuel rod

FRAPCON and FRAPTRAN use a similar representation of the fuel rod geometry: The rod is treated as an axisymmetric structure, which reduces the governing equations for heat transfer and deformations from three to two dimensions. The equations are further reduced from two (radial-axial) to one (radial) dimension by dividing the fuel rod into a number of axial segments and assuming that there is no axial variation of key properties within individual segments. This is usually referred to as the "quasi 2D" or "1 1/2D" approach [18], which involves solving a set of one-dimensional (radial) thermal-mechanical problems (one for each axial segment) that are only weakly coupled. More precisely, coupling between axial segments involve axial forces within the fuel pellet column and the cladding tube, coolant axial flow, and axial flow of gas along the pellet-cladding gap. For the gas flow, instantaneous axial mixing and pressure equilibration is assumed by default in FRAPCON and FRAPTRAN, but there is a simple optional model for delayed pressure equilibration in FRAPTRAN [17].

2.1.1 Axial segmentation

In FRAPCON and FRAPTRAN, the active (fuelled) part of the rod is divided into an arbitrary number of segments, for which the one-dimensional thermal-mechanical equations are solved. The length of each axial segment may be chosen arbitrarily. The heat generation rate and the coolant conditions are assumed to vary from one segment to another, but the material properties are assumed to be the same for all segments. At the upper end of the fuel rod, a

gas plenum with user-defined volume is always assumed to be present. At the lower end, a similar gas plenum volume may be modelled in FRAPTRAN, if needed.

For a number of discrete time steps that together make up the fuel operating history to be studied, the temperature distribution and the pellet and cladding deformations are calculated together with the fuel fission gas release for each of the axial segments separately. In each time step, iterations are usually needed to reach convergence with regard to the properties that couple the axial segments, i.e. pellet and cladding axial forces, coolant properties and rod internal gas pressure. Hence, the computational procedure in FRAPCON and FRAPTRAN is strongly linked to the axial segmentation of the fuel rod active length. For this reason, it is natural to make use of the same segmentation when incorporating an algorithm for axial gas flow and mixing in these programs. In the gas flow model, the internal gas volume in each axial segment can be treated as a finite volume, the properties of which are given by the segment's geometry, temperature distribution and fission gas release rate, as calculated by the host code.

The fuel rod gas plenum is represented by a single axial segment in FRAPCON and FRAPTRAN, and the gas within the plenum volume is assumed to have uniform temperature, pressure and composition. This segmentation may be too crude for use in the model for axial gas flow and mixing. Testing of the model shows that the plenum, containing the major part of the rod's total free gas inventory, must be divided into a number of smaller partial volumes in order to capture the sharp concentration gradients that often arise at the boundary between the gas plenum and the active length of the fuel rod.

2.1.2 Gas volumes within each axial segment

The gas inventory in each axial segment along the fuel rod active length is in FRAPCON and FRAPTRAN assumed to reside in five or six partial volumes [16, 17]:

1. Gas in the pellet-cladding radial gap, including pellet chamfers and the surface roughness.
2. Gas in pellet cracks.
3. Gas in open porosity.
4. Gas at pellet axial dishes.
5. Gas at pellet axial interfaces (excluding dish volumes).
6. Gas in the pellet central hole, in case of annular pellets.

The reason for dividing the gas inventory into these partial volumes is that they may have very different temperature. The temperature differences are considered in calculations of the gas pressure; see section 2.2.2 below. The fuel rod plenum is not divided into partial volumes, since the plenum gas is assumed to have uniform temperature.

2.2 Properties of fuel rod gas inventory

2.2.1 Gas composition

In FRAPCON and FRAPTRAN, the fuel rod is assumed to be fabricated with an initial fill gas consisting of any mixture of He, Ar, Kr, Xe, N₂, H₂, H₂O and air. Under fuel operation, the initial fill gas composition may change by models for release of nitrogen (present in the fuel from fabrication) and the gaseous fission products Xe, Kr and He. The release of these gases is calculated in each axial segment of the fuel rod separately, using the fuel local conditions as input for the calculations. However, in the present versions of FRAPCON and FRAPTRAN [16, 17], the locally released gas is assumed to immediately mix with the entire free gas inventory in the fuel rod, meaning that the gas composition is treated as uniform in the entire fuel rod.

2.2.2 Gas temperature and pressure distribution

In each axial segment along the fuel rod active length, the gas in the partial volumes defined in section 2.1.2 are assumed to have the following temperature [16, 17]:

1. Gas in the pellet-cladding radial gap is assumed to be at the average of the pellet outer and cladding inner surface temperatures.
2. Gas in pellet cracks is assumed to be at the fuel pellet volume average temperature.
3. Gas in open porosity is assumed to be at the fuel pellet volume average temperature.
4. Gas at pellet axial dishes is assumed to be at the fuel pellet volume average temperature.
5. Gas at pellet axial interfaces is assumed to be at the average between the pellet average temperature and the pellet surface temperature.
6. Gas in the pellet central hole (if any) is assumed to be at the fuel pellet centre temperature.

In FRAPCON and FRAPTRAN, the gas pressure in the n :th axial segment is calculated from the total amount (mol) of gas in the segment and the above partial gas volumes and assumed temperatures through the ideal gas law

$$p^n = \frac{\mathcal{N}^n R}{\sum_{k=1}^6 V_k/T_k}, \quad (1)$$

where p^n and \mathcal{N}^n are the gas pressure and total amount of free gas in the n :th segment, R is the universal gas constant, and V_k and T_k refer to gas volumes and temperatures in the six partial volumes considered by FRAPCON and FRAPTRAN in each segment along the fuel pellet column. Equation (1) is derived from the condition of a common pressure in the six partial volumes within the axial segment.

In FRAPCON, the gas pressure is assumed to be uniform not only within each axial segment, but within the entire fuel rod. The sum in equation (1) is thus taken over all partial volumes in all axial segments, including the fuel rod plena, and the amount of gas \mathcal{N} is the total free gas inventory in the rod. This assumption is made also in FRAPTRAN by default, but FRAPTRAN has a simple optional model for delayed pressure equilibration between the upper plenum and the rest of the gas inventory [17]. Hence, the model considers a uniform pressure in the upper plenum and another uniform pressure in the rest of the rod. Time dependent equilibration of these two pressures is calculated by use of the Hagen-Poiseuille equation for viscous flow along part of the pellet-cladding gap [17].

2.2.3 Properties of the flowing gas

When evaluating fundamental properties of the flowing and diffusing gas, such as gas viscosity and diffusivity, it is not obvious what gas temperature should be used for evaluating these properties. Henceforth, we assume that, of the six partial gas volumes defined in section 2.1.2, only gas in the pellet-cladding gap, the central hole and in pellet cracks is readily available for axial flow. Fundamental gas properties are therefore calculated based on the volumetric average temperature of this gas.

3 Governing equations for gas flow and mixing

In the following sections, the fundamental equations that govern axial transport and mixing of the fuel rod gas inventory are presented.

3.1 Basic assumptions and notation

The gas within the cladding tube is assumed to be at sufficiently low pressure that it obeys the ideal gas law. However, the equation of state for the ideal gas must be somewhat modified, in order to take the inhomogeneous gas temperature distribution within the finite volumes into account, as described in section 2.2.2.

Due to differences between the axial segments in heat generation rate, fuel burnup and the resulting deformations of pellets and cladding, the fuel rod flow channel geometry can not be considered entirely one-dimensional: the cross sectional area of the flow channel will vary slightly along the fuel rod. For this reason, the flow of gas inside the fuel rod is assumed to be quasi-one dimensional:

- The variation in flow channel cross sectional area along the fuel rod is taken into account in the governing gas dynamic equations.
- The flow is assumed to be entirely axial and the lateral variation in axial velocity over the flow channel cross sectional area is neglected.

The theory of quasi one-dimensional flow of compressible fluids is well established, and could be studied in e.g. [19].

The bulk flow of gas is modelled by solving the equations for conservation of mass and momentum, as described in sections 3.3 and 3.4. The equation for conservation of energy is neglected, which means that the model does not consider any changes in gap gas temperature caused by the axial flow of gas. Such changes have been observed just after cladding rupture in some LOCA simulation tests on short-length rodlets, when comparatively cool gas flows rapidly from the plenum to the cladding breach in the hot part of the rodlet [12]. However, in most situations, this effect can be neglected.

The equations for conservation of mass and momentum are applied in integral form. The advantage with integral conservation equations is seen when they are applied to quasi one-dimensional flow: they are nicely reduced to algebraic equations, relating properties at different cross-sections of the flow channel with the rate of change in mass or momentum.

The equations governing multicomponent diffusion are presented in section 3.5. Since the theory of multicomponent diffusion is quite complicated, it would certainly need a report on its own. The fundamental equations are given, together with the simplifying assumptions needed to practically and numerically solve the problem. The contribution from thermal diffusion is neglected [20], which means that the model does not consider axial temperature gradients as a driving force for the diffusion; only concentration gradients in the multicomponent gas mixture are considered.

Finally, the equations governing the outflow of gas from a leaking fuel rod are described in section 3.6. They are used for calculating the outflow rate as a function of leak size, gas temperature and rod internal overpressure.

In the equations that follow below, superscripts will be used to indicate a certain finite volume, whereas subscripts will be used to indicate a certain gas constituent. Properties without any subscript refer to the total amount of gas, comprising all constituents. Hence, ρ_i^n denotes molar density of the i :th gas species in volume n , whereas ρ^n denotes the total (bulk) molar density of gas in the same volume.

3.2 Equation of state for the gas

The equation of state used in the gas mixing algorithm is the ideal gas law, which in its general form reads

$$pV = \mathcal{N}RT. \quad (2)$$

Here, p is the gas pressure, V the gas volume and \mathcal{N} the amount of gas in moles. R is the universal gas constant, and T the absolute temperature of the gas. An ideal gas is a gas where all inter-molecular forces are neglected.

Equation (2) is extensively used in the gas mixing algorithm. For the implementation in FRAPCON and FRAPTRAN, the pressure in finite volumes along the active (fuelled) length of the fuel rod is actually calculated from equation (1), in order to capture the inhomogeneous temperature distribution of the gas within these volumes.

3.3 Equation for conservation of mass

The change in gas mass per unit time for a finite volume is governed by the net inflow of mass and the net production rate of mass within that volume. This law for conservation of mass is applied to the bulk of gas, as well as to individual components in the gas mixture.

3.3.1 Bulk flow of gas

In general, the conservation of mass within an arbitrary volume V with a boundary surface A requires that

$$\frac{\partial}{\partial t} \int_V \rho dV = \int_V (q - d) dV - \int_A \rho \bar{u} \cdot d\bar{s}, \quad (3)$$

where ρ is the gas molar density (molm^{-3}), q and d are the volumetric gas production and depletion rates ($\text{mol}(\text{m}^3\text{s})^{-1}$), and \bar{u} is the gas flow velocity (ms^{-1}). The first term in the right-hand-side of equation (3) represents the change in mass due to production and depletion of gas, whereas the second term represents net outflow of mass through the boundary of the volume.

Considering a fixed volume V^n as in Figure 1, with flow only in the axial direction, equation (3) reduces to

$$\int_{V^n} \left(\frac{\partial \rho^n}{\partial t} - q^n + d^n \right) dV = J^{n-1} - J^n, \quad (4)$$

where J are the molar flows (mols^{-1}) in the axial direction, defined by the unit vector \bar{e}_z

$$J = A \rho \bar{u} \cdot \bar{e}_z. \quad (5)$$

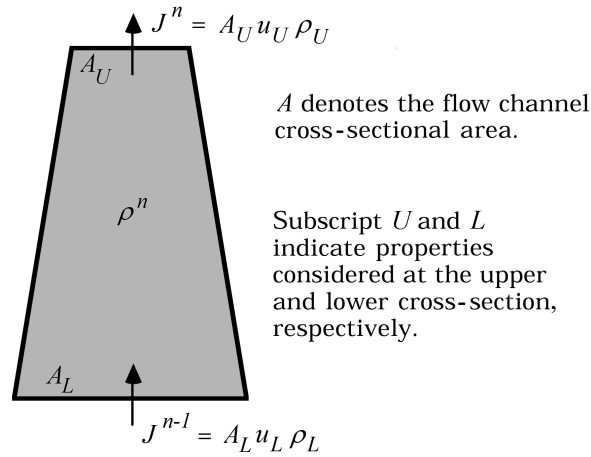


Figure 1: Mass conservation in a fixed finite volume V^n with quasi one-dimensional flow.

3.3.2 Flow of individual gas species

The mass conservation equation for individual gas species, which in the following text are indicated by subscript i , will be somewhat different from equations (3) and (4). The difference is found in the outflow term, where the diffusive interchange of gas across the boundary surface must be taken into account. More precisely, the mass balance for the i :th gas species is

$$\frac{\partial}{\partial t} \int_V \rho_i dV = \int_V (q_i - d_i) dV - \int_A (\rho_i \bar{u} + \bar{j}_{di}) \cdot d\bar{s}, \quad (6)$$

where \bar{j}_{di} denotes the diffusive molar flux ($\text{mol}(\text{m}^2\text{s})^{-1}$) of the i :th gas component. We note that there can be a diffusive flux, even though the flow velocity is equal to zero. In this case, there will be no net transport of mass out of the volume, only interchange of individual gas constituents that tend to reduce gradients in the global gas composition. In the quasi one-dimensional flow geometry, the mass balance will be

$$\int_{V^n} \left(\frac{\partial \rho_i^n}{\partial t} - q_i^n + d_i^n \right) dV = J_i^{n-1} + J_{di}^{n-1} - J_i^n - J_{di}^n, \quad (7)$$

where J_{di} are the axial molar flows (mols^{-1}) of the i :th gas component due to diffusion

$$J_{di} = A \bar{j}_{di} \cdot \bar{e}_z. \quad (8)$$

3.4 Equation for conservation of momentum

The second fundamental equation is for conservation of momentum, stating that the change in momentum per unit time for a gas is equal to the sum of forces acting on it.

3.4.1 Bulk flow of gas

In the gas mixing algorithm, all gases in the multicomponent mixture are assumed to flow with the same axial velocity in the presence of axial pressure gradients. The momentum equation for this bulk flow of gas is

$$\frac{\partial}{\partial t} \int_V m \rho \bar{u} dV = - \int_A p d\bar{s} - \int_A (m \rho \bar{u}) \bar{u} \cdot d\bar{s} - \int_V \bar{f}_f \rho dV, \quad (9)$$

where the new parameters m , p and \bar{f}_f are the molar mass (kgmol^{-1}) of the gas mixture, gas pressure (Pa) and volumetric forces (Nm^{-3}). The volumetric forces \bar{f}_f may contain contributions from wall friction, gravity and other external forces acting on the gas. Since gravity gives a negligible axial pres-

sure gradient in the fuel rod geometry, only the flow channel wall friction is considered in the following.

3.4.2 Flow resistance from wall friction

Since the only volumetric force considered in our model is the wall friction, the last term in equation (9) may be expressed by the shear stress, τ_f (Pa), in the fluid at the flow channel wall

$$\int_V \bar{f}_f \rho dV = \int_L \pi D_p \tau_f dz. \quad (10)$$

Equation (10) is valid for flow in a cylindrical pipe with inner diameter D_p and axial length L . This simple pipe flow is used as a reference case for other, more complicated, flow channel geometries by introducing an equivalent (hydraulic) diameter D_h , defined through

$$D_h = \frac{4A}{P_w}, \quad (11)$$

where A is the cross-sectional area of the flow channel and P_w is the wetted perimeter of the channel, i.e. the perimeter of the wall in contact with the flowing fluid. For a cylindrical pipe with diameter D_p , it follows that $D_h = D_p$. For the fuel rod geometry, assuming that the pellet column is concentrically placed in the cladding tube and surrounded by an annular gas-filled pellet-cladding gap with a radial width of Δr , $D_h = 2\Delta r$.

For laminar flow, the shear stress at the wall, induced by wall friction, is

$$\tau_f = \frac{\eta u \text{Ha}}{8D_h}, \quad (12)$$

where η is the dynamic viscosity (Pas) of the gas and Ha (-) is the nondimensional Hagen number. The latter property is generally dependent on both the flow channel geometry and the fluid velocity. A description of the Hagen number applied in the GAS MIX model is given in appendix A.

Combining equations (10) - (12), the momentum equation (9) can be written

$$\int_V \left(\frac{\partial(m\rho\bar{u})}{\partial t} + \frac{\eta\bar{u}\text{Ha}}{2D_h^2} \right) dV = - \int_A p d\bar{s} - \int_A (m\rho\bar{u})\bar{u} \cdot d\bar{s}. \quad (13)$$

It should be noticed that the volume of integration in equation (13) may be restricted to those parts of the finite gas volume where the gas is mobile and the flow velocity is not equal to zero. For axial flow of gas inside the fuel rod, the last term in equation (13) can be neglected. Due to the obstructive geometry, the flow velocity is generally very low, and the quadratic term in \bar{u} is

generally much smaller than the other terms. With this assumption, equation (13) applied to the quasi one-dimensional flow may be written as

$$\int_L \left(\frac{\partial(mJ)}{\partial t} + \frac{\eta J \text{Ha}}{2\rho D_h^2} \right) dz = - \int_A p d\bar{s} \cdot \bar{e}_z, \quad (14)$$

where J is the axial molar flow (mols^{-1}), and L is the axial length of the volume under consideration. Using the equation of state for the gas, (2), the pressure can be expressed in the molar density and the gas average temperature

$$\int_L \left(\frac{\partial(mJ)}{\partial t} + \frac{\eta J \text{Ha}}{2\rho D_h^2} \right) dz = -R \int_A \rho T d\bar{s} \cdot \bar{e}_z. \quad (15)$$

The expression in equation (15) is used together with equation (4) to calculate the bulk molar flow of gas between axial segments in the fuel rod. The two equations contain the molar density and the molar axial flows as primary unknowns.

3.5 Multicomponent diffusion

In gas mixtures with more than two components, the transport of individual gas constituents due to diffusion is much more complicated than in a binary gas system, for which the diffusive flux of a constituent is dependent only on the concentration gradient of that very component. In a multicomponent system, the diffusive flux of one gas depends also on the concentration gradients of all the other gases present in the system. This cross-dependence is in general rather complicated, and the complexity increases rapidly with increasing number of gas constituents. The presence of axial temperature gradients along the fuel rod also complicates the matter, since the temperature gradients provide a driving force for the diffusion, in addition to the concentration gradients. The phenomenon, which is known as thermal diffusion [20], is neglected in GASMIX. Hence, we consider multicomponent diffusion under uniform temperature and pressure.

The general equations that govern multicomponent diffusion under these conditions are presented in section 3.5.1. In section 3.5.2, a few simplifying assumptions are made about the gas, leading to a more tractable set of equations that are solved numerically in the GASMIX model. These are known as the Stefan-Maxwell (or Maxwell-Stefan) equations, which were developed independently and in parallel by Josef Stefan for fluids and James Clerk Maxwell for dilute gases. Finally, in section 3.5.3, we explore an even more simplified approach to the problem of multicomponent diffusion. This approach, which lends itself for cases where helium is the dominating gas species in the fuel rod free volume, can be used as an option in the GASMIX model.

3.5.1 General equations

The diffusive molar flux ($\text{mol}(\text{m}^2\text{s})^{-1}$) of the i :th component in a mixture with N components may be written [21]

$$\bar{j}_{di} = \frac{\rho^2}{m_i RT \rho_m} \sum_{k=1}^N m_i m_k \mathcal{D}_{ik} \left(f_k \sum_{l \neq k} \frac{\partial G_k}{\partial f_l} \nabla f_l \right), \quad (16)$$

where ρ_m is the gas mass density (kgm^{-3}) of the gas mixture, m_i are the molar masses (kgmol^{-1}) of the constituents, f_i are their molar fractions (-), and G_i are their partial molar free enthalpies (Jmol^{-1}). Moreover, the diffusivities \mathcal{D}_{ik} in equation (16) are the Curtiss-Hirschfelder multicomponent diffusivities [22]. These diffusivities are asymmetric, i.e. $\mathcal{D}_{ik} \neq \mathcal{D}_{ki}$, and they depend on the composition of the gas mixture. Simplifications of equation (16) are needed to obtain a numerically tractable problem.

3.5.2 Stefan-Maxwell equations

A simplified approach to treat diffusion in multicomponent systems is possible if the following requirements are met:

- The gas is at low pressure, which means that the molecular interaction is low. This in turn means that the diffusivities of the components can be considered independent of the molar composition of the system.
- The diffusion occurs under conditions of uniform temperature and pressure, which means that the driving force for the diffusion consists solely of the concentration gradients for the gas constituents.

If these conditions are satisfied, then equation (16) can be simplified to the Stefan-Maxwell equations, which have the following form [22, 23]

$$\sum_{k=1, k \neq i}^N \frac{f_i \bar{j}_{dk} - f_k \bar{j}_{di}}{D_{ik}} = \nabla \rho_i, \quad (17)$$

where D_{ik} are the well-known binary diffusion coefficients. When these are assumed to be independent of the molar composition of the gas mixture, the system of equations given by (17) becomes linear and easy to solve for the diffusive molar fluxes \bar{j}_{di} . The expressions used for calculating the binary diffusivities in the GASMIX model are presented in appendix B. In its current implementation, GASMIX treats gas mixtures with up to ten constituents.

In a one-dimensional system consisting of only two gas constituents, equation

(17) can be written explicitly as

$$\begin{aligned}\frac{f_1 j_{d2} - f_2 j_{d1}}{D_{12}} &= \frac{\partial \rho_1}{\partial z}, \\ \frac{f_2 j_{d1} - f_1 j_{d2}}{D_{21}} &= \frac{\partial \rho_2}{\partial z}.\end{aligned}$$

From this system of equations, it is clear that the Stefan-Maxwell equations are singular. Additional information is thus needed to determine the diffusive molar fluxes. This information is provided by the fact that there is no bulk transport of mass by diffusion alone, i.e.

$$\sum_{i=1}^N j_{di} = 0. \quad (18)$$

The system of linear equations given by (17) and (18) is the default set of equations solved in the GASMIX algorithm for determining the diffusive molar fluxes across finite volume boundary surfaces. An optional set of equations can be solved for certain cases; see below.

3.5.3 Simplified equations

Considering the fact that, in sound (non-leaking) fuel rods with low burnup and/or low fission gas release, helium will be the dominating gas constituent in the fuel rod void volumes, the cross-correlation with other gases than helium can be neglected when calculating the diffusive molar fluxes of e.g. xenon and krypton. In other words, the molar flux of each gas constituent can be calculated as if it were the only gas present in a matrix of helium. The simple equations of binary diffusion is then applicable

$$\bar{j}_{di} = -D_{i\text{He}} \nabla \rho_i. \quad (19)$$

This can also be derived from the Stefan-Maxwell equations, by setting all molar fractions to zero except for helium, whose molar fraction is set equal to unity. The molar flux of helium is then found from the additional condition in equation (18)

$$\bar{j}_{d\text{He}} = - \sum_{i \neq \text{He}}^N \bar{j}_{di}, \quad (20)$$

or in the one-dimensional case considered for the fuel rod

$$j_{d\text{He}} = - \sum_{i \neq \text{He}}^N j_{di}. \quad (21)$$

In the GASMIX algorithm, the user may choose to calculate the diffusive molar fluxes either through the Stefan-Maxwell equations or the simplified equations described above. The Stefan-Maxwell equations are valid for any composition of gases, whereas in the simplified method, helium is assumed to be the main component.

3.6 Outleakage of gas through a cladding breach

To simulate outleakage of gas through a cladding breach, GASMIX uses a model based on one-dimensional isentropic¹ flow of a calorically perfect gas. Under these conditions, simple relations between the state of the outleaking gas inside (subscript i) and outside (subscript o) of the cladding apply; see Figure 2. More precisely, the conservation equations for mass and energy of the gas that passes through the breach can be written

$$\rho_i u_i = \rho_o u_o, \quad (22)$$

$$h_i + \frac{u_i^2}{2} = h_o + \frac{u_o^2}{2}, \quad (23)$$

where u and ρ denote the gas velocity and density. The enthalpy, h , for a calorically perfect gas depends only on temperature through $h = c_p T$, where the specific heat capacity c_p is assumed to be constant [19].

We seek a relation for the unknown outflow velocity u_i by combining equations (22) and (23) and using this simple expression for the enthalpy, which results in

$$u_i^2 \left(1 - \left(\frac{\rho_i}{\rho_o} \right)^2 \right) = 2c_p T_i \left(\frac{T_o}{T_i} - 1 \right). \quad (24)$$

Next, we express the unknown ratios of densities and temperatures in equation (24) with known ratios for the pressure, by use of well-known relations for isentropic flow of ideal gases [19]

$$\begin{aligned} \frac{T_o}{T_i} &= \left(\frac{p_o}{p_i} \right)^{\frac{\gamma-1}{\gamma}}, \\ \frac{\rho_i}{\rho_o} &= \left(\frac{p_i}{p_o} \right)^{\frac{1}{\gamma}}, \end{aligned}$$

where $\gamma = c_p/c_v$ is the heat capacity ratio. We note that $\gamma \approx 1.66$ for monoatomic gases, ≈ 1.40 for air and hydrogen, and ≈ 1.32 for steam. By substituting these relations into equation (24), we find an expression for u_i in terms

¹Isentropic means that the flow is adiabatic (no heat exchange) and reversible (no energy transformation due to friction or dissipative effects).

of the known gas temperature T_i and the known pressures p_i and p_o

$$u_i = \sqrt{\frac{2c_p T_i p_o^\beta (p_i^\alpha - p_o^\alpha)}{p_i^\alpha (p_i^\beta - p_o^\beta)}}, \quad (25)$$

where the coefficients are defined by $\alpha = (\gamma - 1)/\gamma$ and $\beta = 2/\gamma$. Equation (25) is used in GASMIX for calculating the velocity of outflowing gas, in case a cladding breach is postulated in any of the axial segments along the fuel rod. The molar depletion rate d_i^n ($\text{mol}(\text{m}^3\text{s})^{-1}$) of a specific gas constituent i from the finite volume n with volume V^n is then calculated from

$$d_i^n = u_i \rho_i^n A_{cb} / V^n, \quad (26)$$

where ρ_i^n is the molar density of the gas constituent and A_{cb} is the area of the cladding breach. The latter is currently expected to be given as input by the user, together with the axial position of the leak; see section 5.2. However, when the GASMIX model is implemented as part of the FRAPTRAN program, these parameters are expected to be calculated by the models for cladding rupture in the host code.

Finally, we note that only outflow ($p_i > p_o$) may be modelled, because of the simplifying assumption of isentropic flow of a calorically perfect gas. Modelling the ingress of steam into a fuel rod would, in principle, be possible. However, it would require a more sophisticated inflow model, taking the phase transition from liquid water to steam into account.

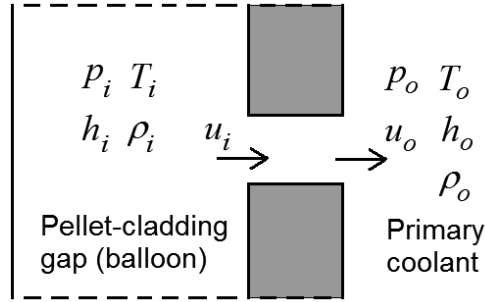


Figure 2: Isentropic outflow of gas through a postulated cladding breach.

4 Numerical solution of the gas flow equations

In this section, a numerical solution method to the fundamental equations expounded in section 3 is presented. From the fundamental equations for conservation of mass and momentum and multicomponent diffusion, the evolution of the molar densities ρ_i^n is determined for each finite volume n in an implicit time stepping scheme, where fission gas release and thermal properties of the fuel rod gas inventory serve as time dependent input to the calculations. The strategy for solving the incremental change in gas molar distribution during a timestep is as follows:

1. Find the change in axial bulk molar flow at the boundary surfaces to each of the finite volumes in the discretized rod geometry. This is done by simultaneously solving the one-dimensional conservation equations for mass (4) and momentum (15) over the time step.
2. Determine the interchange of gas species between the finite volumes, due to bulk flow and diffusion across the volume interfaces. This is done by solving the Stefan-Maxwell equations (optionally the simplified equations in section 3.5.3) and the componental form of the conservation equation for mass, i.e. equation (7).

These two steps are thoroughly described in the following subsections.

4.1 Determination of bulk molar flow

4.1.1 Spatial discretization of the conservation equations

Under the assumption of quasi one-dimensional flow, the equation for conservation of mass reduces to the simple form in equation (4). The momentum equation (15) can be numerically treated in two different ways. The first option is to transform the equation into a finite difference relation. This route is applied in most fuel performance codes with gas flow models, leading to a relation for the molar flows J^n of the form

$$\frac{\partial(\bar{m}J^n)}{\partial t} + \frac{\bar{\eta}J^n\bar{\text{Ha}}}{2\bar{\rho}\bar{D}_h^2} = -\frac{RA_U(\rho^{n+1}T^{n+1} - \rho^nT^n)}{\Delta z}. \quad (27)$$

The bars in equation (27) indicate values taken as some interpolated average at the boundary between volume n and $n+1$. The inertia effects, represented by the first left-hand side term, can in most cases be neglected in the fuel rod flow, since the pressure and friction terms are usually many orders of magnitude

greater than the time derivative. However, in scenarios that involve rapid rod depressurization following cladding rupture or burst-type release of fission gas under reactivity initiated accidents, the inertia effects may be important. In the GASMIX algorithm, the time derivative in equation (27) has been kept to allow modelling of these events. This also allows an implicit time stepping scheme to be applied when solving the equation.

Equation (27) will lead to correct results, as long as there are no abrupt changes in the flow channel properties between axial segments. Unfortunately, there are such changes, more precisely at the interfaces between gas plena and the fuel column. These discontinuities can of course be explicitly taken into account when evaluating molar flows through equation (27), but it is simpler to abandon the finite difference technique in favour of the second solution method. This method, which is applied in the GASMIX algorithm, involves evaluating the integrals in equation (15) at the finite volume interfaces. The volume of integration must then be located at the interface of two successive axial segments. Figure 3 shows the volumes of integration that are used in GASMIX when discretizing the equations for conservation of mass and momentum, respectively. With this discretization, equation (4) will remain unchanged

$$\left(\frac{\partial \rho^n}{\partial t} - q^n + d^n \right) V^n = J^{n-1} - J^n. \quad (28)$$

The momentum equation (15) yields

$$\begin{aligned} & \left(\frac{\partial(m^n J^n)}{\partial t} + \frac{\eta^n \lambda^n J^n}{\rho^n} \right) \frac{L^n}{2} + \\ & \left(\frac{\partial(m^{n+1} J^n)}{\partial t} + \frac{\eta^{n+1} \lambda^{n+1} J^n}{\rho^{n+1}} \right) \frac{L^{n+1}}{2} = RA_U^n (\rho^n T^n - \rho^{n+1} T^{n+1}), \end{aligned} \quad (29)$$

where the following parameters are used:

$$A_L^n = \min(A^n, A^{n-1}), \quad (30)$$

$$A_U^n = \min(A^n, A^{n+1}), \quad (31)$$

$$\lambda^n = (\text{Ha}/2D_h^2)^n. \quad (32)$$

The free cross-sectional flow area at the finite volume boundary is thus set to the minimum area of the two interfacing axial segments. The parameter λ^n can be interpreted as a geometric flow resistance factor. As can be seen from the expression used for the Hagen number, given in appendix A, λ^n is strongly dependent on the hydraulic diameter

$$\lambda^n \approx \left(\frac{1}{D_h^n} \right)^{3.6}. \quad (33)$$

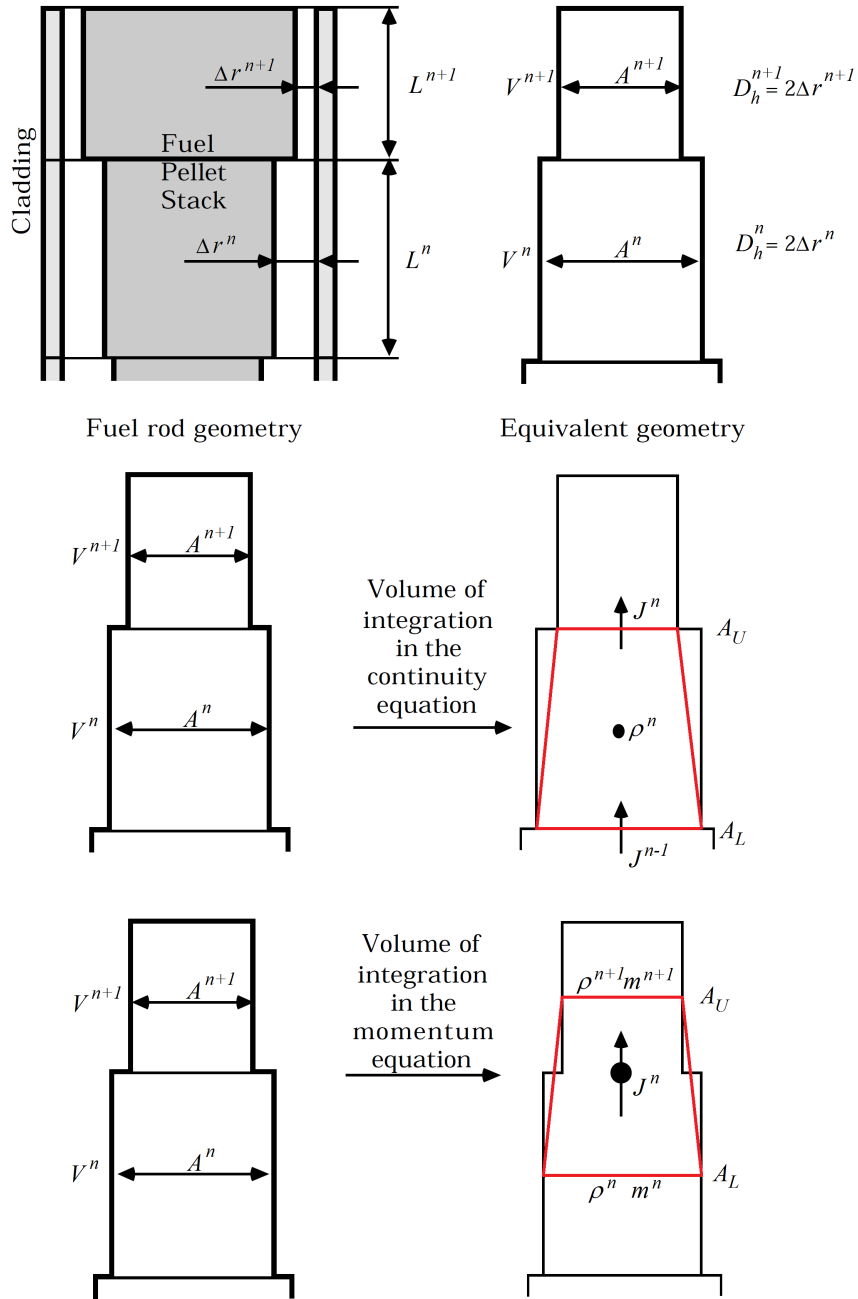


Figure 3: Spatial discretization of the quasi one-dimensional equations for conservation of mass and momentum in GASMIX.

4.1.2 Temporal discretization of the conservation equations

Equations (28) and (29) must also be discretized with respect to time. This is in GASMIX done by applying the generalized midpoint rule, sometimes also called the θ -method. According to this method, the first order differential equation $\partial x/\partial t = f(x)$ may be approximated by the finite difference

$$\frac{x(t + \Delta t) - x(t)}{\Delta t} = f(x(t + \theta\Delta t)), \quad (34)$$

where $x(t + \theta\Delta t)$ in the right-hand-side function f is evaluated by linear interpolation

$$x(t + \theta\Delta t) = (1 - \theta)x(t) + \theta x(t + \Delta t). \quad (35)$$

The parameter θ may be chosen in the range $[0,1]$. Any value of θ greater than zero will result in an implicit time integration scheme, thus requiring iterations for its solution. Values of θ equal to or greater than 0.5 result in an unconditionally stable time stepping scheme, which is needed for efficient solution of equations (28) and (29).

Some well-known time integration schemes are found as special cases for certain values of θ :

$\theta = 0.0$: Forward Euler method, fully explicit,

$\theta = 1.0$: Backward Euler method, fully implicit,

$\theta = 0.5$: Crank-Nicolson method.

4.1.3 Fully discretized conservation equations

By discretizing all time derivatives according to equation (34), equations (28) and (29) result in two interconnected systems of nonlinear equations, where the molar density and the bulk molar flow in each of the finite volumes at time $t + \Delta t$ are the unknowns to be determined. By collecting these unknowns in arrays, henceforth denoted $\bar{\rho}(t + \Delta t)$ and $\bar{J}(t + \Delta t)$, the two systems of equations can be concisely written as

$$\bar{F}(\bar{\rho}(t + \Delta t), \bar{J}(t + \Delta t)) = \bar{0}, \quad (36)$$

$$\bar{G}(\bar{\rho}(t + \Delta t), \bar{J}(t + \Delta t)) = \bar{0}, \quad (37)$$

where each component in the arrays represents a finite volume (axial segment) in the discretized fuel rod geometry. \bar{F} contains the mass conservation equation (28) for each finite volume, whereas \bar{G} represents the momentum conservation equation (29). These functions form the basis for the numerical solution of the conservation equations. Because of their importance, they are given in explicit form in appendix C.

4.1.4 Application of Newton-Raphson iterations

The system of nonlinear equations defined by (36) and (37) is in GASMIX solved iteratively by use of the Newton-Raphson method [24]. By this method, a nonlinear system of equations that is formally given by

$$\bar{f}(\bar{x}) = \bar{0} \quad (38)$$

is solved by iterations, in which the unknowns \bar{x} are incrementally corrected in each iteration until equation (38) is approximately satisfied. The corrective increments in the k :th iteration step are found by solving a system of linear equations

$$\bar{\mathfrak{J}} \cdot \delta\bar{x}_k = \bar{f}(\bar{x}_{k-1}), \quad (39)$$

where the Jacobian matrix $\bar{\mathfrak{J}}$ contains the partial derivatives of \bar{f} , evaluated by use of values for the unknowns \bar{x} from the previous iteration step

$$\bar{\mathfrak{J}} = \left(\frac{\partial \bar{f}}{\partial \bar{x}} \right)_{\bar{x}=\bar{x}_{k-1}}. \quad (40)$$

Before passing to the next iteration step, the unknowns are corrected

$$\bar{x}_k = \bar{x}_{k-1} - \delta\bar{x}_k. \quad (41)$$

The iterations are terminated when all components of the corrective increments $\delta\bar{x}_k$ have decreased to less than a specified maximum value.

In GASMIX, the Newton-Raphson method is applied to simultaneously solve the discretized conservation equations for mass (36) and momentum (37), which are given in explicit form in appendix C. Hence, with respect to the above nomenclature, we identify \bar{x} , \bar{f} and $\bar{\mathfrak{J}}$ from

$$\bar{x} = \begin{bmatrix} \bar{\rho}(t + \Delta t) \\ \bar{J}(t + \Delta t) \end{bmatrix}, \quad (42)$$

$$\bar{f} = \begin{bmatrix} \bar{F} \\ \bar{G} \end{bmatrix}, \quad (43)$$

$$\bar{\mathfrak{J}} = \begin{bmatrix} \frac{\partial \bar{F}}{\partial \bar{\rho}} & \frac{\partial \bar{F}}{\partial \bar{J}} \\ \frac{\partial \bar{G}}{\partial \bar{\rho}} & \frac{\partial \bar{G}}{\partial \bar{J}} \end{bmatrix}. \quad (44)$$

Each of the four blocks in the Jacobian matrix has a bi-diagonal or diagonal form, where the elements depend on geometrical properties of the flow channel, current molar densities and the current molar flows at volume interfaces. In the numerical implementation of the GASMIX algorithm, the calculations

of the Jacobian and the residual functions \bar{F} and \bar{G} are performed in separate subroutines; see appendix D. The corrective increments $\delta\bar{x}$ are then obtained by applying a suitable standard solver to the linear system of equations in (39). In this way, the core of the solution algorithm is made fairly modular and tractable with standard solvers for sparse systems of linear equations.

4.2 Redistribution of gas constituents

Redistribution of individual components in the gas mixture can be calculated as soon as the axial bulk molar flow and the diffusive flows have been determined. Equation (7) is applied for this purpose, where the molar densities of each constituent in each finite volume at the advanced time, $\rho_i^n(t + \Delta t)$, are the unknowns. When applying this equation, the partial molar flows due to the bulk flow of gas, J_i , must be calculated with consideration of the axial flow direction. If the molar fraction of gas constituent i in the n :th finite volume is denoted by f_i^n , the partial molar flow is defined by

$$\begin{aligned} J_i^n &= J^n f_i^{n+1} \quad \text{if } J^n < 0, \\ J_i^n &= J^n f_i^n \quad \text{if } J^n > 0. \end{aligned} \tag{45}$$

This algorithm has been successfully tested in GASMIX. Tests have shown that, if instead *averaged* values of the partial molar fractions at the finite volume interface are used in calculating J_i^n , the algorithm tends to break down in case of steep gradients in gas composition.

Apart from this peculiarity in calculating the component molar flows, and the addition of diffusive flows, the flow of individual components can be treated in the same manner as the bulk flow. A vectorial residual function \bar{H} is thus defined for each of the gas components

$$\bar{H}(\bar{\rho}_i(t + \Delta t)) = \bar{0}. \tag{46}$$

The explicit expressions for the components H_i^n of this function are given in appendix C. With these residuals, a system of equations for the unknowns $\rho_i^n(t + \Delta t)$ may then be solved with the Newton-Raphson technique presented in section 4.1.4. Instead of solving one large system of equations, GASMIX simplifies the problem by solving one linear system of equations with only N_{VOL} unknowns for each component in the gas mixture separately. This technique is further described in section C.2, appendix C.

4.3 Criterion on convergence in iterations

A suitable criterion for defining when the solution of the gas flow equations has converged is inherent in the Newton-Raphson method. The criterion is based on the maximum norm of the corrective increments for the molar distribution of individual gas species, here denoted $\delta\bar{\rho}_i$. This array contains N_{VOL} elements, one for each finite volume in the discretized flow channel. Convergence is considered to be reached in iteration number k , if the following condition is satisfied

$$\max_{n,i} \left(\frac{|\delta\bar{\rho}_i^k|}{\bar{\rho}_i^k + \bar{\rho}_i^{k-1}} \right) \leq \varepsilon_\rho. \quad (47)$$

Here, ε_ρ is a user-defined preset parameter, suitably chosen in the order of 10^{-5} . Please notice that superscript k in equation (47) in this case denotes the current step of iteration, not a certain finite volume. The maximum is taken over all finite volumes (n) and gas species (i).

5 The GASMIX set of subroutines

The algorithms and models presented in section 4 and appendices A to C have been numerically implemented in a set of FORTRAN subroutines and functions, intended for incorporation into the FRAPCON and FRAPTRAN fuel performance analysis programs [16, 17]. The top-level subroutine, which controls the presented algorithms, is named GASMIX. It is supposed to be repeatedly called from FRAPCON and FRAPTRAN, more precisely in each time step taken by these codes as a specific irradiation history is analysed.

As mentioned in section 2, the spatial discretization of the governing equations for gas flow and mixing follows the axial segmentation of the active (fuelled) part of the fuel rod used in FRAPCON and FRAPTRAN. Also the "global" time stepping in the gas calculations is imposed by these host codes, although the global time steps may be divided into shorter internal sub-steps within GASMIX to ensure accuracy and convergence when solving the equations for gas flow and mixing. In each of the global time steps taken by FRAPCON or FRAPTRAN, the GASMIX algorithm will compute the change in gas molar distribution. Hence, GASMIX will solve the problem schematically shown in Figure 4. The current implementation of GASMIX supports the calculation of multicomponent flow for systems with up to ten gas species. The gases supported by the model are: He, Kr, Xe, H₂, O₂, H₂O, N₂, Ar, CO and CO₂.



Figure 4: Purpose of the GASMIX subroutine. Here, t_{beg} and t_{end} refer to the time at beginning and end of a global time step in FRAPCON or FRAPTRAN.

The GASMIX subroutine consists of three major blocks:

1. Setting of initial data at $t = t_{beg}$. Input is obtained from other computational modules of the host code, e.g. relating to the flow channel geometry, fission gas release and gas temperature.
2. Solving of the gas flow equations in section 4. An internal time stepping scheme is utilized, making the algorithms independent of the global time step length used by the host code.
3. Creating output of the gas state at $t = t_{end}$, in a form accepted by other program modules in the host code. Output consists primarily of

the calculated distribution of each gas constituent and the gas pressure distribution.

A detailed presentation of the GASMIX subroutine and its subordinate routines and functions is given in appendix D. The main features are outlined in the following sections.

5.1 Flowchart of the GASMIX subroutine

A complete flowchart of the GASMIX subroutine is given in appendix D, together with descriptions of subordinate routines and functions. In Figure 5, a top level map of GASMIX with its most important parts is presented. The three main blocks of the routine are clearly seen from Figure 5, together with the loops for internal time stepping and Newton-Raphson iterations.

5.2 User-defined input to GASMIX

A number of options is available in the GASMIX subroutine, allowing the user to control the gas mixing calculations. These options, which are defined in Table 1, are read supposed to be from the `$frpcon` block in the input file to FRAPCON-QT-4.0 and the `$model` block in the input file to FRAPTRAN-QT-1.5. All input parameters are optional: if they are not defined in the input files, the default values defined in Table 1 are used.

Table 1: Optional input parameters that control the GASMIX algorithm. The default value within brackets [] is used in case the parameter is not specified in the input file.

Parameter:	Value:	Meaning:
<code>igmix</code>	[0] 1	Gas flow and mixing is not considered. The GASMIX algorithm is activated.
<code>idiff</code>	[0] 1 2	Gas diffusion is not considered. Gas diffusion is considered with simplified equations. Gas diffusion is considered with Stefan-Maxwell equations.
<code>nlpls</code>	[1]	Number of finite volumes used for discretizing the fuel rod lower gas plenum (if any).
<code>nupls</code>	[1]	Number of finite volumes used for discretizing the fuel rod upper gas plenum.
<code>ileak</code>	[0]	A cladding leak will be modelled in finite volume number <code>ileak</code> . Zero means no leak.
<code>aleak</code>	[0.0]	Area of the cladding breach (m ²), in case a cladding leak is modelled.
<code>gasmp</code>	[1.0]	Parameter θ in the generalized midpoint rule; see equation (34). $\theta \in [0, 1]$.

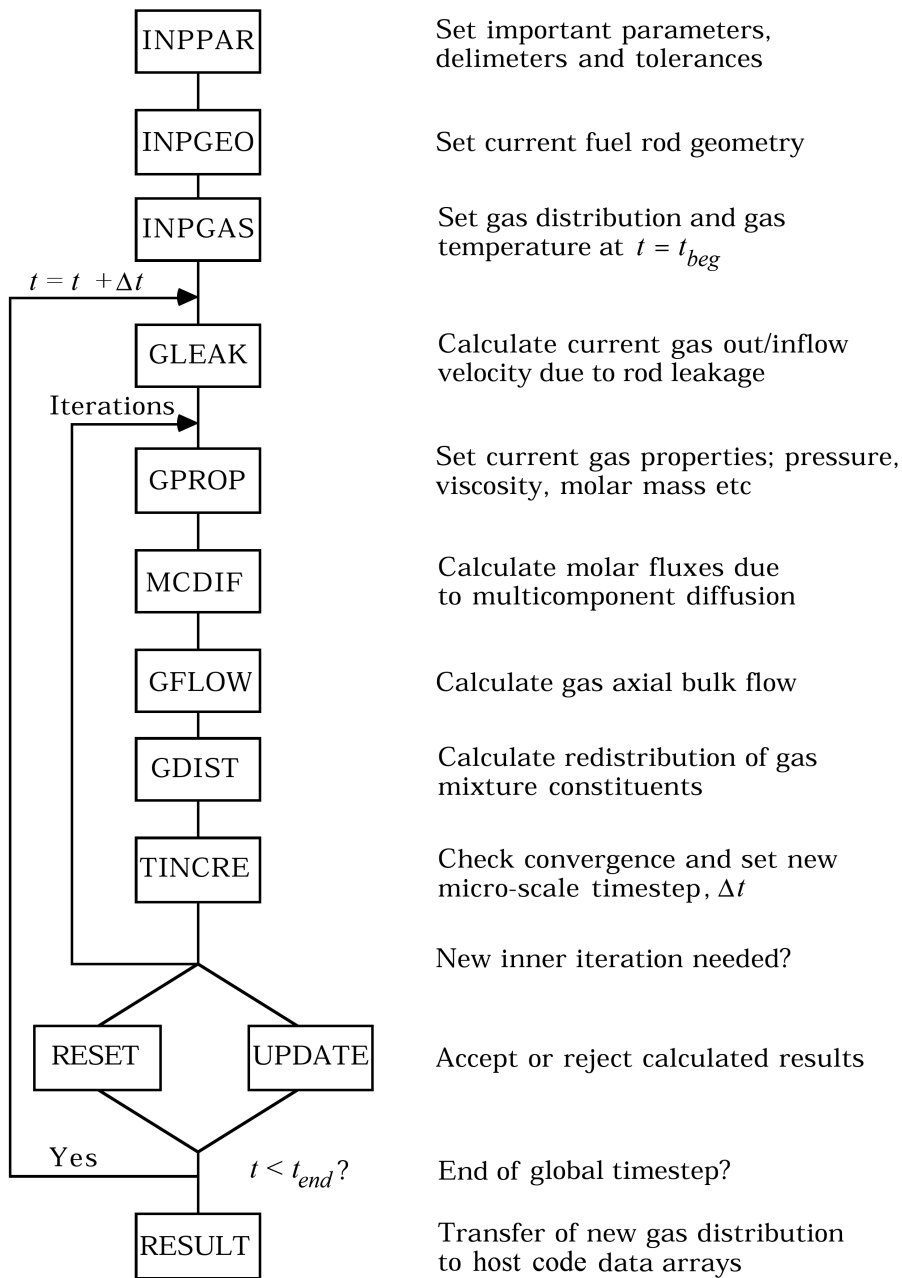


Figure 5: Top-level flowchart of the GASMIX subroutine, which controls the calculations for gas flow and mixing. A complete flowchart, comprising also lower-level subroutines and functions, is presented in appendix D.

6 Model verification and validation

The correctness of the numerical implementation of the GASMIX algorithm has been verified by comparing calculated results with analytical solutions of simple problems. The models have also been validated against a limited number of experiments. The testing has been done with GASMIX as a stand-alone computational module, i.e. before introducing the source code into the FRAPCON and FRAPTRAN host codes.

Some examples of the testing are given below. In section 6.1, a simple analytical solution for one-dimensional binary diffusion is used in order to confirm that the model correctly reproduces diffusive gas mixing. In section 6.2, a gas flow experiment performed in the 1970s on a PWR fuel rod with a burnup of about $25 \text{ MWd}(\text{kgU})^{-1}$ is used for validating the model with regard to its capacity to reproduce bulk flow of gas induced by axial pressure gradients.

6.1 Gas mixing by diffusion

6.1.1 Analytical reference case

An analytical solution to a simple problem of one-dimensional binary diffusion under uniform temperature and pressure was used in order to verify the calculation of axial diffusive transport of gas constituents in the fuel rod. The considered reference case is illustrated in Figure 6: A tube with length L , open in both ends, contains gas with a molar density of $C_0 \text{ molm}^{-3}$ at time $t = 0$. The open tube is surrounded by another gas, which has the same molar density and pressure as the gas inside the tube. The concentration of the gas inside the tube will follow Fick's second law of diffusion

$$\frac{\partial^2 C}{\partial z^2} - \frac{1}{D} \frac{\partial C}{\partial t} = 0, \quad (48)$$

where D is the binary diffusion coefficient for the two gases involved. The initial condition is $C(z, t = 0) = C_0$ and the idealized boundary conditions are $C(z = 0, t) = C(z = L, t) = 0$. An analytical solution to equation (48) with these initial and boundary conditions can be found by separation of variables, i.e. by seeking a solution with the form $C(z, t) = \mathcal{Z}(z) \times \mathcal{T}(t)$. With this ansatz, an analytical solution in the form of an infinite trigonometric series can be found [25]

$$C(z, t) = \frac{4C_0}{\pi} \sum_{n=0}^{\infty} \frac{1}{2n+1} \sin\left(\frac{(2n+1)\pi z}{L}\right) \exp\left(-\frac{(2n+1)^2 \pi^2 D t}{L^2}\right). \quad (49)$$

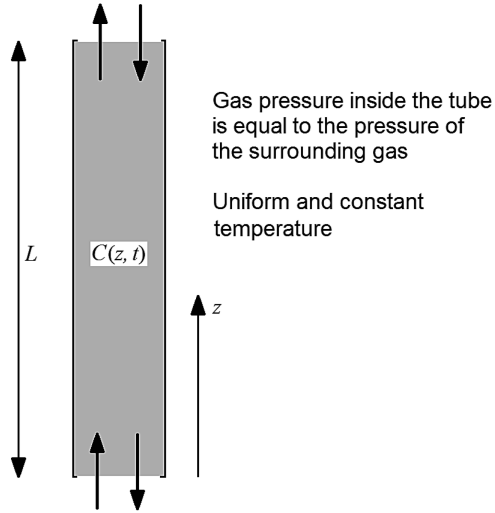


Figure 6: One-dimensional diffusion in a tube with open ends is considered for model verification.

For the purpose of model verification, equation (49) was implemented in a simple FORTRAN program and used as a reference solution. The infinite sum was truncated after the first 200 terms.

6.1.2 Computational modelling

The one-dimensional geometry in Figure 6 was approximately modelled in GASMIX. The tube was represented by a fuel rod, divided into 24 axial segments with equal length along its active (fuelled) part. This part was assumed to be initially filled with helium. The open ends were simulated by modelling very large lower and upper gas plena, initially filled with argon. Each plenum was modelled with a single finite volume. The geometry was fully symmetric, with uniform temperature and pressure. The conditions modelled in GASMIX are summarized in Table 2.

Table 2: Conditions modelled in GASMIX for the test case with one-dimensional diffusion.

Property:		Value:
Fuel pellet column length	[mm]	3650.0
Fuel pellet outer diameter	[mm]	9.200
Cladding tube inner diameter	[mm]	9.260
Lower gas plenum volume	[m ³]	0.100
Upper gas plenum volume	[m ³]	0.100
Gas pressure	[MPa]	0.098
Gas temperature	[K]	293.0
He-Ar binary diffusivity	[mm ² s ⁻¹]	77.026

The diffusive mixing of the gas was calculated with the GASMIX model. The global time stepping was given a fixed step length of 500 seconds, and the molar distribution in the fuel rod was recorded for each of these time steps up to a final time of 50 000 seconds. The calculated results were compared with the analytical solution given by equation (49).

6.1.3 Results

Figure 7 shows the gradual decrease in helium concentration at the rod centre position. The calculated concentration is in very good agreement with the analytical solution in equation (49). Obviously, the diffusive dilution of He is a very slow process at room temperature; still after 50 000 seconds (13.9 hours), there is roughly 10 % of helium left at the fuel rod centre position.

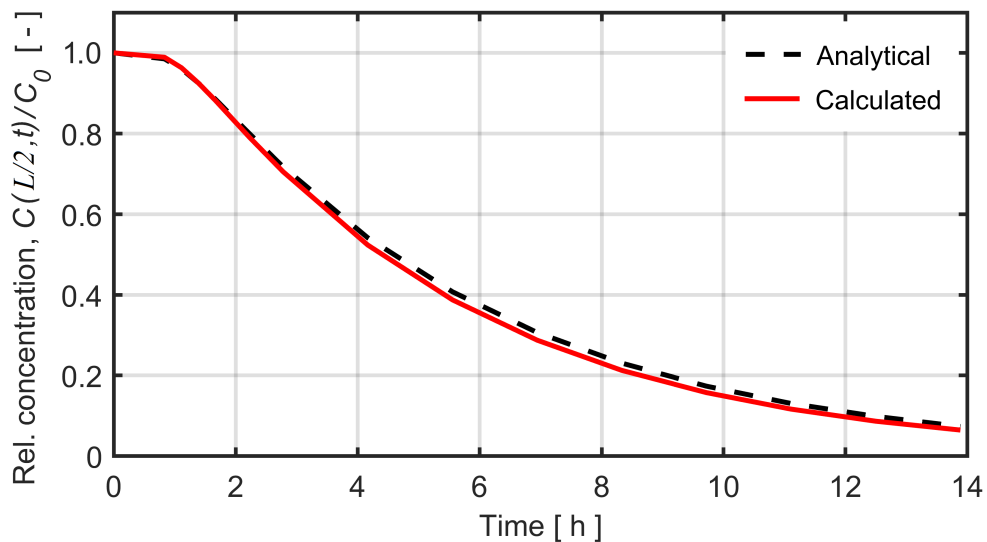


Figure 7: Decrease in helium concentration at the rod centre position ($z = L/2 = 1825$ mm).

Figure 8 shows the axial distribution of helium at time $t = 10\,000$ seconds (2.8 hours). Also in this case, the agreement with the analytical solution is good. The major difference is found at the fuel rod centre position. The agreement would probably have been better if the active part of the fuel rod had been divided into a greater number of axial finite volumes than 24. The calculated axial distribution of helium is perfectly symmetric with respect to the fuel rod centre.

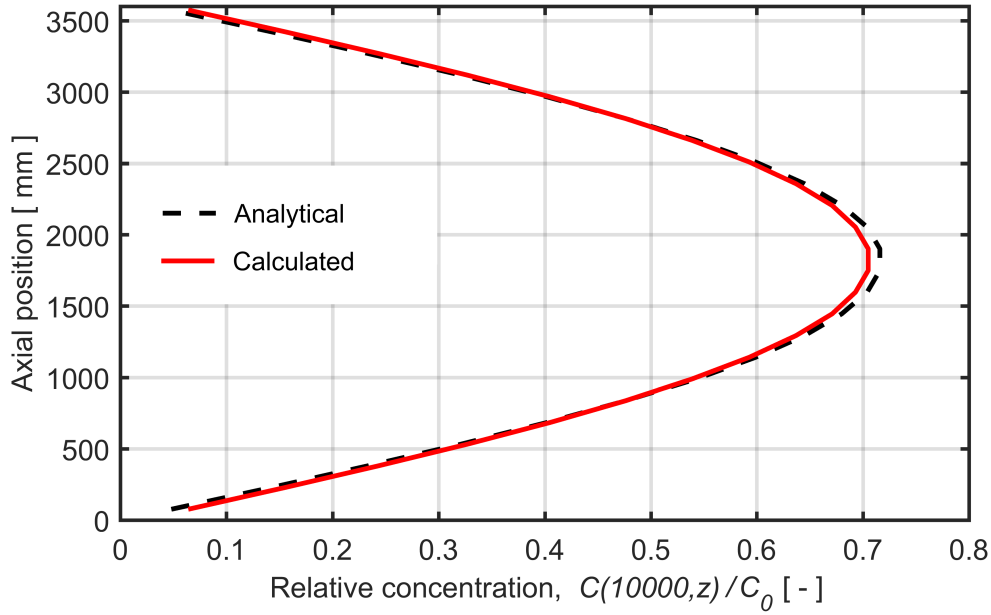


Figure 8: Axial profile for the helium concentration at time $t = 10\,000$ s (2.8 h).

6.2 Gas flow due to pressure gradients

6.2.1 The INEL gas flow experiments

In the mid-1970s, a series of experiments on axial gas flow in irradiated PWR fuel rods were performed at Idaho National Engineering Laboratory (INEL). The main purpose of the experiments was to investigate the influence of pellet-cladding gap width and pellet cracks on the flow resistance in irradiated fuel rods [10]. Both steady and transient gas flow was studied. The steady gas flow experiments were conducted by letting gas at a well-determined rate flow from the top to the bottom of the fuel rod, while measuring the pressure drop along the fuel rod by use of nine pressure transducers applied at different axial positions. The transient gas flow experiment consisted of a highly pressurized PWR fuel rod that was punctured in the bottom end. The decrease in gas pressure was then recorded as a function of time by a pressure transducer, located in the top of the fuel rod.

The INEL steady gas flow experiments were conducted on six full-length fuel rods that had been irradiated to a rod average burnup around $25 \text{ MWd}(\text{kgU})^{-1}$ in a commercial PWR. One of these rods, named K4 in [10], was thoroughly investigated by destructive examination. The gas flow path was determined by studying the pellet-cladding gap and the pellet crack pattern at six different cross-sections of the fuel rod. The pellet-cladding radial gap width, Δr , varied between 9 and $55 \mu\text{m}$, depending on axial and azimuthal position. The

number of major pellet cracks per section varied from 3 to 13, and their size varied from narrow fissures ($0.5 \mu\text{m}$ wide) to large cracks ($130 \mu\text{m}$ wide). Grinding and re-polishing the sample revealed that the crack pattern in the fuel pellet was substantially altered over $< 1 \text{ mm}$ axial distance and was completely changed over approximately 1 cm . Hence, the flow paths made up of pellet cracks were extremely tortuous.

Here, we will consider six experiments with steady gas flow. All of them were carried out on rod K4, the internal geometry of which was thoroughly characterized in post-test destructive examinations. A steady gas flow from the upper gas plenum to the bottom of the fuel rod was attained by connecting the two ends of the rod to large vessels, containing gas at different pressures. The steady molar flow rate was measured, and the pressure drop over the fuel rod was determined with the aid of nine pressure transducers, connected to the rod at different axial positions. Tests were performed with both helium and argon, and the experiments were conducted both at room temperature and at 533 K ; in the latter case, the fuel rod was heated with a furnace.

6.2.2 Computational modelling

The geometry of rod K4 was modelled in GASMIX. Key properties of the rod geometry are listed in Table 3, and the axially varying pellet-cladding gap used in the computations is shown in Figure 9. The assumed gap width variation in Figure 9 is based on the data reported for six axial positions in [10].

Six of the steady gas flow tests on rod K4 were modelled with GASMIX. The molar flow rate and exit pressure in each considered test are given in Table 4. All of these tests were conducted at 298 K .

Table 3: Conditions modelled in the INEL K4 gas flow tests [10].

Property:		Value:
Fuel pellet column length	[mm]	3650.0
Fuel pellet outer diameter	[mm]	9.300
Cladding tube inner diameter	[mm]	9.465
Cladding tube outer diameter	[mm]	10.705
Lower gas plenum volume	[cm^3]	12.200
Upper gas plenum volume	[cm^3]	12.200
Gas temperature	[K]	298.0

The experiments in Table 4 were modelled with GASMIX by prescribing a steady inflow of either helium or argon to the uppermost axial segment of the rod, while keeping the lowest axial segment at constant pressure. The inflow rate and exit pressure were set equal to the values given in Table 4. It

should be noticed that a steady gas flow was reached roughly one minute after the injection of gas into the upper plenum was started. As before, the active length of the rod was discretized into 24 equal-length axial segments for the calculations.

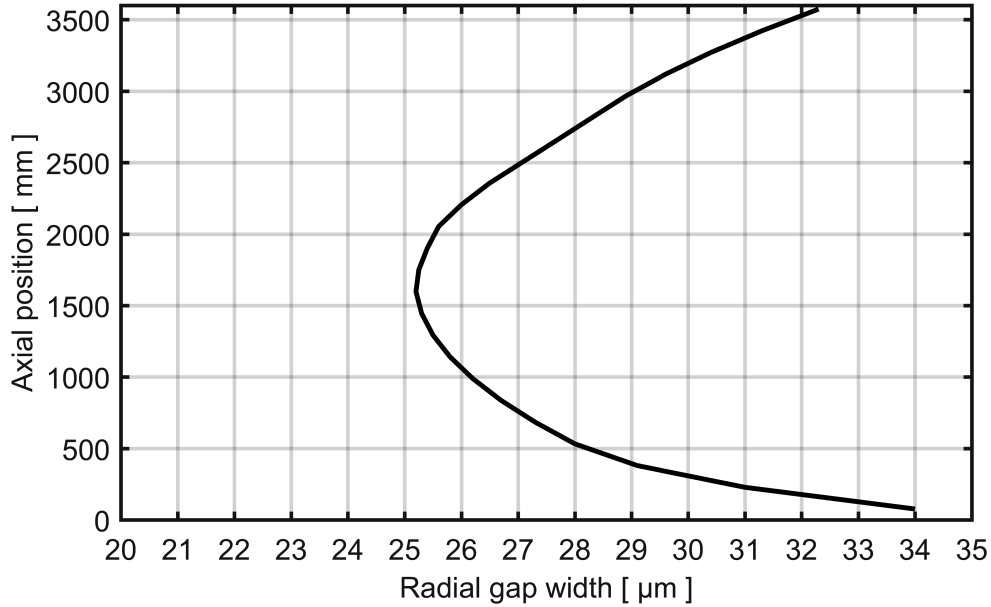


Figure 9: Room-temperature pellet-cladding radial gap width assumed for fuel rod K4, based on data in [10].

Table 4: INEL K4 steady gas flow tests modelled with GASMIX [10]. All tests were conducted at 298 K.

Test nr	Gas	Molar flow [mmols ⁻¹]	Exit pressure [MPa]
1	He	0.43	2.39
2	He	1.27	3.51
3	He	0.93	5.27
4	Ar	0.38	2.18
5	Ar	0.98	3.48
6	Ar	0.68	5.16

6.2.3 Results

The axial pressure distribution calculated by GASMIX was compared to the experimental results given in [10]. The calculated axial pressure distributions are given in Figures 10 and 11, together with experimental data from each of the tests. The agreement is fair for all investigated flow rates and pressures in both helium and argon. The discrepancies are presumably due to differences in the axial variation of pellet-cladding gap width between the GASMIX model and the actual fuel rod.

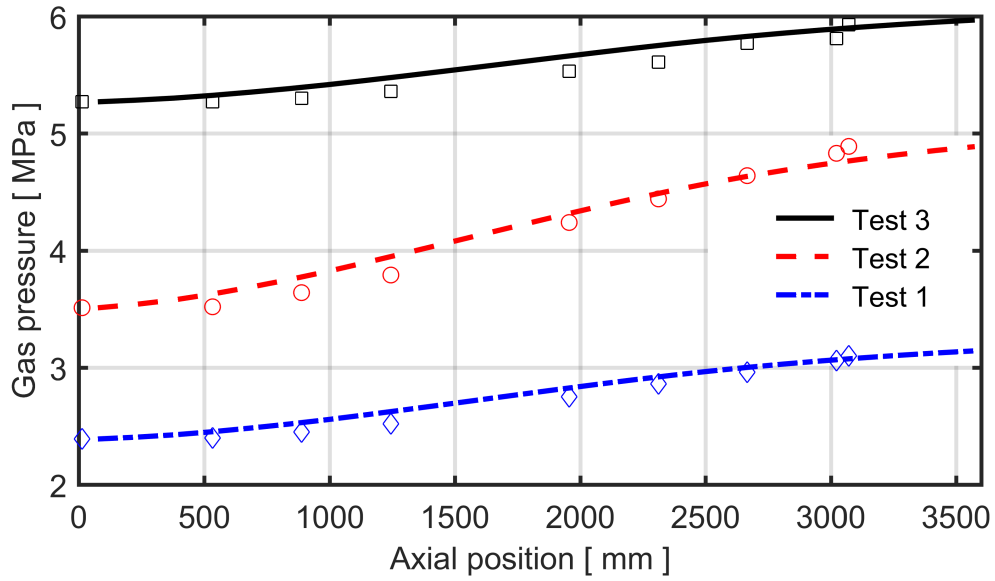


Figure 10: Steady flow of helium at 298 K. Markers are experimental data for tests 1-3 [10], lines are gas pressures calculated by GASMIX.

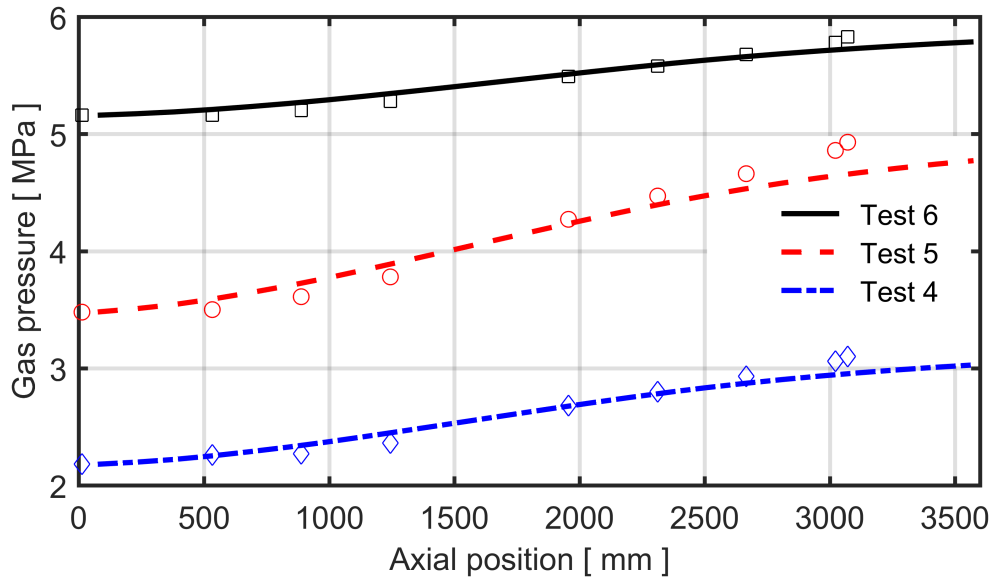


Figure 11: Steady flow of argon at 298 K. Markers are experimental data for tests 4-6 [10], lines are gas pressures calculated by GASMIX.

7 Conclusions and outlook

The computational model for axial gas flow and mixing presented in this report is intended for analyses of a wide spectrum of operating conditions for light water reactor fuel rods, ranging from normal reactor operation to severe accident scenarios. The model, named GASMIX, captures multicomponent gas flow due to axial pressure gradients as well as diffusion; two phenomena with very different time scales. This makes the model different from gas transport models used in existing fuel rod analysis programs, which are aimed to model either fast pressure equilibration under accident conditions [17, 26] or slow diffusive mixing under normal operating conditions [27].

The versatility of the model is a result of simultaneously solving the equations for conservation of mass and momentum of the gas and the Stefan-Maxwell equations for multicomponent diffusion. The approach is believed to be particularly well suited for modelling axial transport and mixing of the fuel rod gas inventory under load-follow operation, where axial flow of gas due to pressure gradients, arising from frequent power changes, is expected to interact with diffusive processes.

The governing equations are discretized with respect to space and time by use of standard methods, leading to a system of non-linear equations to be solved in each time step of the operating history under study. The solution methods are numerically implemented in a set of FORTRAN subroutines and functions, intended for incorporation into the FRAPCON and FRAPTRAN fuel rod analysis programs [16, 17]. The equations are discretized in space by use of a quasi one-dimensional finite volume model of the pellet-cladding gap and other internal free volumes of the fuel rod. This discretization is chosen, since it fits the axial segmentation used in many fuel rod analysis programs that apply a so-called "quasi-2D" or "1 1/2D" approach for solving the governing equations for heat transfer, fission gas release and mechanical equilibrium. The intended host codes for the presented gas flow and mixing model, FRAPCON and FRAPTRAN, belong to this category of programs. The resulting interconnected systems of equations are solved with respect to time by use of an efficient, implicit, time stepping scheme, in which the Newton-Raphson method is used for internal iterations. Fuel rod deformations, fission gas release and temperature of the fuel rod gas inventory serve as space-time dependent input to the calculations, provided by the host code.

Outleakage of gas through a cladding breach with postulated area can be modelled at an arbitrary axial position of the fuel rod. The gas outflow rate through the cladding breach is calculated based on the gas temperature and the rod internal overpressure. The calculations are done by an ancillary model, using theory for isentropic flow of a calorically perfect gas to describe the gas that flows out through the breach. Modelling the ingress of steam into a failed fuel rod would, in principle, be possible. However, it would require a more so-

phisticated model for the inflowing water or steam, taking the phase transition from liquid water to steam into account.

The implemented model was verified against a simple analytical solution for one-dimensional binary diffusion. Excellent agreement was found between the calculated results and the analytical solution, which indicates that the numerical implementation is correct. However, it should be made clear that the case under study is a simplified benchmark problem that does not necessarily represent diffusion in operating fuel rods. For example, Killeen and Haaland [3] observed a much slower diffusion in the Halden IFA-504 in-reactor gas mixing experiments than expected from theory. From the experiments, they derived an "effective" binary diffusivity for helium and argon that was about an order of magnitude lower than reported in literature. They attributed the unexpectedly slow diffusion in the operating fuel rod to the tortuous flow path that the diffusing gas has to traverse, due to misaligned pellets and pellet cracks. Based on the aforementioned effective binary diffusivity, they concluded that this tortuous flow path was about three times longer than expected from the axial distance along the pellet-cladding gap in the test rod [3]. It is therefore recommended to analyse the IFA-504 experiment [3, 4] with GASMIX, in order to determine an empirical "tortuosity reduction factor", by which the ideal binary diffusion coefficients in appendix B should be multiplied.

Studies should also be undertaken to investigate the importance of axial temperature gradients to the diffusion. The GASMIX model does not consider temperature gradients as a driving force for the diffusion; only concentration gradients in the multicomponent gas mixture are considered. The contribution from thermal diffusion in gases with moderate temperature gradients is usually small, but experimental data [28] suggest that the contribution may be fairly large in He-Xe and He-Kr mixtures, due to the significant differences in atomic mass for these gas pairs.

The GASMIX model was also validated against a series of steady gas flow experiments on a PWR fuel rod with a rod average burnup around $25 \text{ MWd}(\text{kgU})^{-1}$ [10]. The experiments were conducted by letting room-temperature helium or argon flow from the top to the bottom of the fuel rod at well-determined rates, while measuring the pressure drop along the fuel rod by use of nine pressure transducers applied at different axial positions. The model reproduces the measured pressure drop in these experiments with fair accuracy. The discrepancies are believed to result from uncertainties in the pellet-cladding gap width used in the modelling. Post-test metallographic examinations, carried out on six different cross-sections of the test rod, showed that the pellet-cladding radial gap width varied between 9 and 55 μm , depending on axial and azimuthal position. This variation was idealized in the GASMIX computations.

Further analyses of gas flow experiments are warranted, in particular on high-burnup fuel rods with small or entirely closed pellet-cladding gaps. A few suitable experiments have been conducted within Part III of the Studsvik Cladding Integrity Project (SCIP-III) [29] and further experiments of this kind are planned for Part IV of the project. The experiments are done by imposing a steady gas flow through short-length test rodlets, prior to LOCA simulation tests. These steady gas flow experiments are valuable for calibration of the correlations for Hagen number and cross-sectional flow area in GASMIX (see appendix A), since they can be modelled with greater exactitude than the transient gas flow that follows upon cladding rupture in the actual LOCA tests.

Acknowledgment This work was funded by the Swedish Radiation Safety Authority (SSM) under contract number SSM2018-4296.

References

- [1] R. J. White, E. Skattum, and A. Haaland. Communication of fission products in the interior of a fuel rod, with particular emphasis on recent tests on the IFA-430 gas flow rig. Report HPR-325, OECD Halden Reactor Project, Halden, Norway, 1985.
- [2] J. C. Killeen and A. Haaland. Mixing of argon and helium in the interior of a fuel rod: results of experiments with the IFA-504 gas flow rig. Report HWR-172, OECD Halden Reactor Project, Halden, Norway, 1986.
- [3] J. C. Killeen and A. Haaland. Mixing of argon and helium in the interior of an operating fuel rod. Report HWR-186, OECD Halden Reactor Project, Halden, Norway, 1986.
- [4] J. C. Killeen. Thermal response of the gas flow rig IFA-504 to fission gas release. Report HWR-194, OECD Halden Reactor Project, Halden, Norway, 1987.
- [5] C. Vitanza, T. Johnsen, and J. M. Aasgaard. Interdiffusion of noble gases: results of an experiment to simulate dilution of fission gases in a fuel rod. Report HPR-295, OECD Halden Reactor Project, Halden, Norway, 1983.
- [6] M. Kinoshita. Axial transport of fission gas in LWR fuel rods. In *IAEA Specialists Meeting on Water Reactor Fuel Element Performance Modelling*, IWGFPT/13, pages 387–396, Preston, UK, March 15-19, 1982. IAEA.
- [7] M. Kinoshita. Evaluation of axial fission gas transport in power ramping experiments. *Res Mechanica*, 19(3):219–226, 1986.
- [8] N. Kjaer-Pedersen. The effect of axial diffusional delays on the overall fission gas release. In *IAEA Specialists Meeting on Water Reactor Fuel Element Performance Modelling*, IWGFPT/13, pages 343–346, Preston, UK, March 15-19, 1982. IAEA.
- [9] M. T. del Barrio and L. E. Herranz. Axial fission gas transport in nuclear fuel rods. *Defect and Diffusion Forum*, 283-286:262–267, 2009.
- [10] S. J. Dagbjartsson, D. E. Owen, B. A. Murdock, and P. E. MacDonald. Axial gas flow in irradiated PWR fuel rods. Report TREE-NUREG-1158, Idaho National Engineering Laboratory, Idaho Falls, ID, USA, 1977.
- [11] W. Wiesenack, L. Kekkonen, and B. Oberländer. Axial gas transport and loss of pressure after ballooning rupture of high burn-up fuel rods subjected to LOCA conditions. In *Proceedings of the International Conference on the Physics of Reactors (PHYSOR'08)*, pages 2987–2992, Interlaken, Switzerland, September 14-19, 2008. Paul Scherrer Institut.

- [12] W. Wiesenack. Summary of the Halden Reactor Project LOCA test series IFA-650. Report HPR-380, OECD Halden Reactor Project, Halden, Norway, 2013.
- [13] OECD/NEA. Report on fuel fragmentation, relocation, dispersal. Report NEA/CSNI/R(2016)16, OECD Nuclear Energy Agency, Paris, France, 2016.
- [14] G. Khvostov, W. Wiesenack, M. A. Zimmermann, and G. Ledergerber. Some insights into the role of axial gas flow in fuel rod behaviour during the LOCA, based on Halden tests and calculations with the FALCON-PSI code. *Nuclear Engineering and Design*, 241:1500–1507, 2009.
- [15] OECD/NEA. Nuclear fuel behaviour under reactivity-initiated accident (ria) conditions. Report NEA No. 6847, OECD Nuclear Energy Agency, Paris, France, 2010.
- [16] K. J. Geelhood, W. G. Luscher, P. A. Raynaud, and I. E. Porter. FRAPCON-4.0: A computer code for the calculation of steady-state, thermal-mechanical behavior of oxide fuel rods for high burnup. Report PNNL-19418, Vol. 1, Rev. 2, Pacific Northwest National Laboratory, Richland, WA, USA, 2015.
- [17] K. J. Geelhood, W. G. Luscher, J. M. Cuta, and I. E. Porter. FRAPTRAN-2.0: A computer code for the transient analysis of oxide fuel rods. Report PNNL-19400, Vol. 1, Rev. 2, Pacific Northwest National Laboratory, Richland, WA, USA, 2016.
- [18] P. Van Uffelen and M. Suzuki. *Comprehensive Nuclear Materials*, volume 3, chapter 3.19 Oxide fuel performance modeling and simulation, pages 535–577. Elsevier, 2012.
- [19] J. D. Anderson. *Modern Compressible Flow with Historical Perspective*. McGraw-Hill, New York, USA, 1982.
- [20] E. A. Mason, R. J. Munn, and F. J. Smith. Thermal diffusion in gases. *Advances in Atomic and Molecular Physics*, 2:33–91, 1966.
- [21] J. O. Hirschfelder, C. F. Curtiss, and R. B. Bird. *Molecular Theory of Gases and Liquids*, pages 441–513. Wiley, 1954.
- [22] R. B. Bird, C. F. Curtiss, and J. O. Hirschfelder. Fluid mechanics and the transport phenomena. *Chemical Engineering Progress Symposium series*, 51:69–85, 1955.
- [23] S. Whitaker. Derivation and application of the stefan-maxwell equations. *Revista Mexicana de Ingenieria Quimica*, 8(3):213–243, 2009.

- [24] V. S. Ryabenkii and S. V. Tsynkov. *A Theoretical Introduction to Numerical Analysis*. Chapman and Hall, CRC Press, New York, USA, 2006.
- [25] J. Crank. *The Mathematics of Diffusion*, chapter 2.3 Method of separation of variables. Clarendon Press, Oxford, UK, 1975.
- [26] A. Moal, V. Georgenthum, and O. Marchand. SCANAIR: A transient fuel performance code, Part one: General modelling description. *Nuclear Engineering and Design*, 280:150–171, 2014.
- [27] M. Suzuki, H. Saitou, Y. Udagawa, and F. Nagase. Light water reactor fuel analysis code FEMAXI-7; Model and structure. Report JAEA-Data/Code-2013-005, Japan Atomic Energy Agency, Tokaimura, Japan, 2013.
- [28] K. E. Grew and T. L. Ibbs. *Thermal Diffusion in Gases*. Cambridge Monographs on Physics. Cambridge University Press, Cambridge, UK, 1952.
- [29] OECD Nuclear Energy Agency. Studsvik cladding integrity project (SCIP-III). <https://www.oecd-neo.org/jointproj/scip-3.html>, 2019.
- [30] M. Reimann. Analytische untersuchung von gasströmung in ringspalten beim aufblähvorgang von zirkaloy-hüllrohren. Report KFK-2280, Kernforschungszentrum Karlsruhe, Karlsruhe, Germany, 1976. (in German).
- [31] R. C. Reid and T. K. Sherwood. *The Properties of Gases and Liquids*. McGraw-Hill, New York, USA, 2 edition, 1966.
- [32] M. Klein and F. J. Smith. Tables of collision integrals for the (m,6) potential function for 10 values of m. *Journal of Research of the National Bureau of Standards - A. Physics and Chemistry*, 72A(4):359–423, 1968.

A Properties of the flow channel geometry

The geometry of the flow channel, which is made up of the pellet-cladding gap and other free volumes inside the fuel rod, affects both the axial bulk flow of gas and the diffusive mixing of individual components in the gas. Large uncertainties exist in how the properties of the flow channel should be characterized and calculated from the information available from a typical host code, i.e. a computer program for thermal-mechanical analyses of the fuel rod. In the GASMIX model, the flow channel is characterized by two properties, the Hagen number and the cross-sectional area, which are calculated from host code results through user-defined functions. This makes it easy for the user to modify the definition of the flow channel properties, in case more accurate models for the flow channel's influence on the gas flow emerge in the future. A description of the presently implemented functions is given below.

A.1 Flow channel Hagen number

The flow resistance from wall friction in a viscous fluid can be expressed by the nondimensional Hagen number. The Hagen number, which can be seen as the ratio of wall friction forces to overall viscous forces in the fluid, is defined through

$$\text{Ha} = f_w \text{Re}, \quad (\text{A.1})$$

where Re is the Reynolds number of the flow, and f_w is a friction factor for the flow channel wall.

The wall friction factor f_w is generally dependent on both the fluid velocity and the surface properties of the channel wall, but for laminar flow, f_w is independent of the surface roughness [30]. This is easy to understand, since in laminar flow, there is no transfer of mass through the thin boundary layer at the wall. For this reason, the fluid outside the boundary layer will not be directly affected by the surface. In the laminar case, it can be shown that the Hagen number is constant and defined entirely by the flow channel geometry.

In the current implementation of the GASMIX model, the axial flow in the fuel rod is assumed to be laminar and the Hagen number is thus dependent only on the fuel rod internal geometry. More precisely, the Hagen number is calculated from the hydraulic diameter D_h through a correlation derived from experimental results presented in [10]

$$\begin{aligned} \text{Ha} &= 890 && \text{if } D_h < 20 \mu\text{m}, \\ \text{Ha} &= 38.4 + \frac{2.146 \times 10^{-5}}{D_h^{1.617}} && \text{if } D_h \geq 20 \mu\text{m}. \end{aligned} \quad (\text{A.2})$$

In the optional gas flow model in FRAPTRAN, a similar correlation, based on the same set of data, is used [17]. This correlation reads

$$\begin{aligned} \text{Ha} &= 1177 && \text{if } D_h < 25.4 \mu\text{m}, \\ \text{Ha} &= 22 + \frac{6.2377 \times 10^{-3}}{D_h^{-2 \times 10^{-5}}} && \text{if } D_h \geq 25.4 \mu\text{m}. \end{aligned} \quad (\text{A.3})$$

In the GASMIX algorithm, correlation (A.2) is implemented as the function HAGEN. Correlations (A.2) and (A.3) are shown graphically below. As can be seen from the figure, the correlations yield practically identical results for hydraulic diameters greater than $50 \mu\text{m}$. For this region, the two correlations are based on the data presented in [10]. These data do not cover hydraulic diameters less than $50 \mu\text{m}$, and the GASMIX correlation in equation (A.2) is therefore calibrated to the experiments presented in section 6.2 for this region. The support for the FRAPTRAN correlation for $D_h < 50 \mu\text{m}$ in equation (A.3) is unknown.

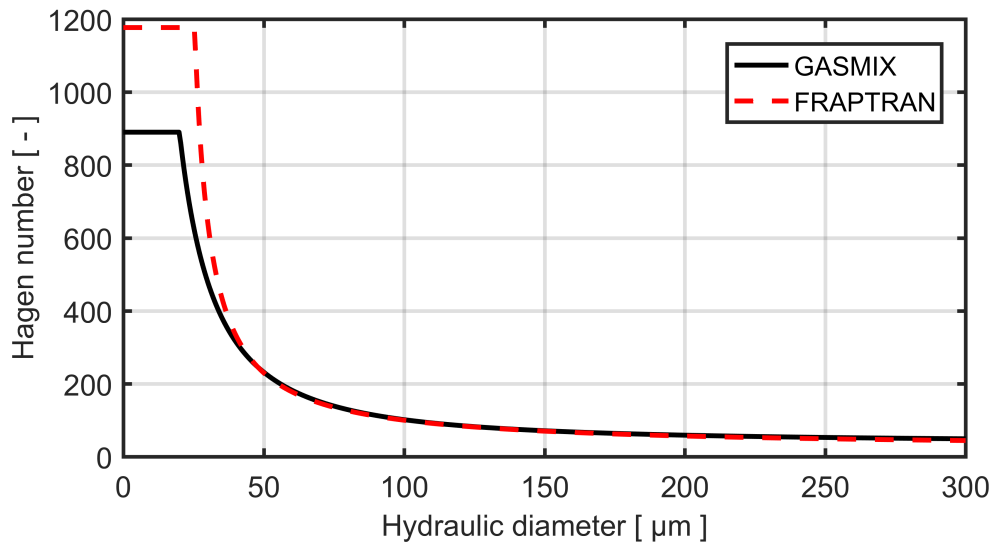


Figure A.1: Hagen number versus hydraulic diameter, calculated through equations (A.2) and (A.3). For hydraulic diameters greater than $50 \mu\text{m}$, both equations are based on data from [10].

A.2 Flow channel cross-sectional area

The most important property of the flow channel is the cross sectional area, leaving a free passage to the flowing gas. When the pellet-cladding gap is closed or nearly closed, it is by no means obvious how this flow area should be defined. Also when the gap is entirely closed, there will be a free passage of gas. This is partly due to the surface roughness of pellet and cladding,

leaving an effective open gap in the order of a few microns. The size of this effective gap can be estimated by measuring the thermal resistance of the pellet-cladding interface. Pellet cracks may also serve as a flow channel for the gas, when the pellet-cladding gap is closed. However, ceramography of cracked fuel pellets show that the flow paths made up of pellet cracks is extremely tortuous, since individual cracks do not generally extend more than a few millimeters in the axial direction [10].

In the GASMIX model, the cross-sectional flow area A is determined by the function `FLAREA` through the expression

$$A = 2\pi\Delta_{eff} \left(R_{ci} - \frac{\Delta_{eff}}{2} \right) \quad (\text{A.4})$$

where the effective gap Δ_{eff} is given by

$$\Delta_{eff} = \Delta_{act} + \sqrt{5} \sqrt{\mathcal{R}_p^2 + \mathcal{R}_c^2} \quad (\text{A.5})$$

Here, R_{ci} is the cladding inner radius, Δ_{act} is the calculated gap size, and \mathcal{R}_p and \mathcal{R}_c are the pellet and cladding surface roughnesses. The effective gap in equation (A.5) is similar to the effective gap used for modelling heat transfer from the pellet to the cladding in thermal calculations. The square root of five stems from averaging the distance between two surfaces with an assumed distribution of irregularities.

B Calculation of binary diffusion coefficients

The diffusion coefficient, sometimes called the diffusivity, is the proportionality constant between the diffusive flux and the gradient of concentration for the diffusing gas in Fick's first law of diffusion. The diffusive molar fluxes for two mixed gases can be written

$$\bar{j}_{d1} = -D_{12} \nabla c_1, \quad (\text{B.1})$$

$$\bar{j}_{d2} = -D_{21} \nabla c_2, \quad (\text{B.2})$$

where \bar{j}_{di} is the diffusive molar flux and ∇c_i is the gradient of the molar density of the i :th gas species. Since no net transport of gas takes place under isobaric diffusion, the above fluxes must for any closed control surface S satisfy the equation

$$\int_S (\bar{j}_{d1} + \bar{j}_{d2}) \cdot d\bar{s} = 0. \quad (\text{B.3})$$

According to kinetic gas theory, the binary diffusion coefficients are independent of the molar densities of the two gas species, and D_{12} and D_{21} will satisfy the condition:

$$D_{12} = D_{21}. \quad (\text{B.4})$$

In practice, the binary diffusion coefficients do vary with concentration. In liquid systems, this variation is large, but for gases at low pressures, the variation of D_{ij} with concentration can usually be ignored. D_{ij} can be calculated through various more or less refined theories. One of the most widely used theories for gases at low pressures are based on the Lennard-Jones expression for the potential energy of nonpolar and spherical molecules [21]

$$V(r) = 4\epsilon_0 \left(\left(\frac{\sigma}{r} \right)^{12} - \left(\frac{\sigma}{r} \right)^6 \right), \quad (\text{B.5})$$

where σ denotes the molecular radius, and ϵ_0 is a constant, specific for the gas species under consideration. Equation (B.5) is known as the Lennard-Jones 12-6 potential. By use of this potential function, the binary diffusion coefficients can be determined through

$$D_{ij} = \frac{C_D T^{3/2}}{p \sigma_{ij}^2 M_{ij} \Omega_D \left(\frac{k_B T}{\epsilon_{ij}} \right)}, \quad (\text{B.6})$$

where p and T are the gas pressure and temperature. Moreover, σ_{ij} , ϵ_{ij} and

M_{ij} are defined by

$$\begin{aligned}\sigma_{ij} &= \frac{\sigma_i + \sigma_j}{2}, \\ \epsilon_{ij} &= \sqrt{\epsilon_i \epsilon_j}, \\ M_{ij} &= \sqrt{\frac{M_i M_j}{M_i + M_j}}.\end{aligned}$$

The properties entering the above expressions are defined in Table B.1.

Table B.1: Properties entering the expressions for the binary diffusion coefficients.

C_D	1.88262×10^{-2}	
k_B	Boltzmann's constant	[JK ⁻¹]
T	Absolute temperature	[K]
p	Gas pressure	[Pa]
M_i	Molecular mass of gas i	[gmol ⁻¹]
σ_i	Molecular radius of gas i	[Angstroem]
ϵ_i	Constant, property of gas i	[Joule]
Ω_D	Collision integral	[-]

The formula in equation (B.6), together with values for σ_i , ϵ_i and Ω_D can be found in [21]. The collision integral Ω_D has the form shown in Figure B.1, where two different sources of information on Ω_D versus the reduced temperature $k_B T / \epsilon_{ij}$ are compared. The correlation used in GASMIX and shown in Figure B.1 is based on tabular data in [31].

Experimentally determined binary diffusion coefficients for a number of gas pairs at different temperatures are given in [21]. In Table B.2, some experimentally determined values of the product pD_{ij} are compared with results obtained from equation (B.6). As can be seen from Table B.2, the calculated values of the binary diffusion coefficients are in good agreement with experimental values. The discrepancies are generally less than 5 %, also for gases with polar or non-spherical molecules.

The current implementation of GASMIX supports the calculation of binary diffusion coefficients for systems with up to ten gas species. The gases supported by the model are: He, Kr, Xe, H₂, O₂, H₂O, N₂, Ar, CO and CO₂.

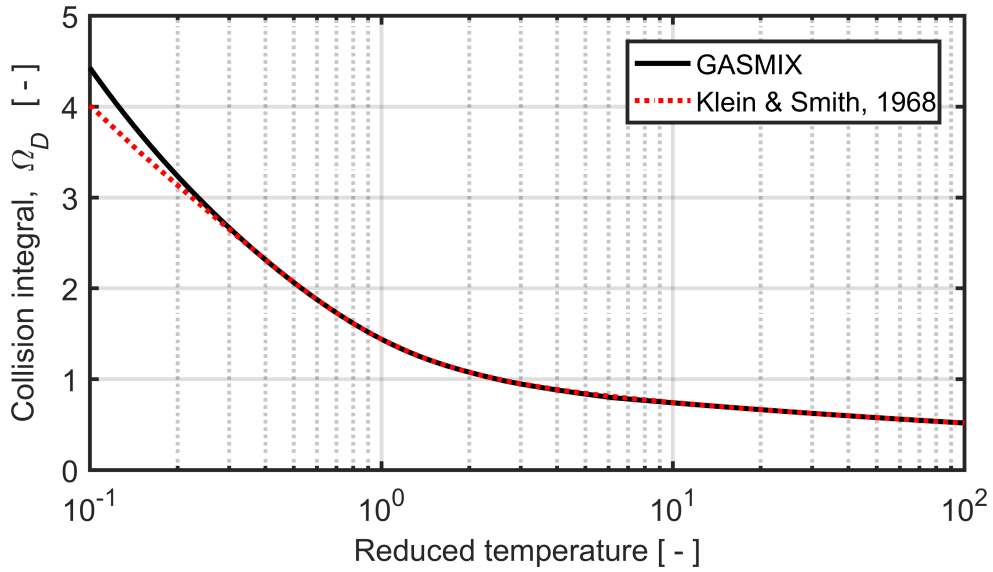


Figure B.1: The collision integral used in GASMIX, based on tabular data in [31], in comparison with tabular data from Klein and Smith [32].

Table B.2: Theoretically evaluated binary diffusion coefficients from equation (B.6) compared with experimentally determined data for relevant binary gas systems [21].

Gas binary system	Absolute temperature [K]	pD_{ij} (Theory, eq. (B.6)) [Ns^{-1}]	pD_{ij} (Experiment) [Ns^{-1}]	Rel error [%]
Ar-He	298.0	0.769	0.729	+6
Ar-Xe	378.0	0.173	0.178	-3
Ar-Kr	276.2	0.124	0.133	-7
Ar-H ₂	242.2	0.538	0.562	-4
Ar-CO ₂	276.2	0.124	0.133	-7
He-N ₂	298.0	0.696	0.687	+1
He-O ₂	298.0	0.779	0.729	+7
He-CO ₂	498.0	1.408	1.414	-1
He-H ₂ O	352.4	1.136	1.121	+1
Xe-H ₂	341.2	0.736	0.751	-2

C Explicit expressions for discretized equations

This appendix presents the space-time discretized equations for conservation of mass and momentum, as solved by the GASMIX algorithm; see sections 4.1.3 and 4.2.

C.1 Bulk flow of gas

By applying the generalized midpoint rule in equation (34) to the spatially discretized conservation equation for mass (28), the elements of the array \bar{F} in equation (36) are found to be

$$F^n (\bar{\rho}(t + \Delta t), \bar{J}(t + \Delta t)) = \rho^n(t + \Delta t) - \rho^n(t) + \Delta t \left(d^n - q^n + \frac{J^n - J^{n-1}}{V^n} \right)_{t=t+\theta\Delta t}. \quad (\text{C.1})$$

All quantities within the large right-hand-side bracket are to be evaluated at the intermediate time $t = t + \theta\Delta t$ through equation (35). Hence, for θ greater than zero, they will contain the unknown molar densities and axial molar flows at $t = t + \theta\Delta t$.

The finite volumes at the top and bottom of the fuel rod must be treated separately, since the axial molar flow at the boundaries is equal to zero. Consequently, for the lowermost finite volume ($n=1$), we have $J^{n-1} = 0$ and

$$F^n (\bar{\rho}(t + \Delta t), \bar{J}(t + \Delta t)) = \rho^n(t + \Delta t) - \rho^n(t) + \Delta t \left(d^n - q^n + \frac{J^n}{V^n} \right)_{t=t+\theta\Delta t}. \quad (\text{C.2})$$

Likewise, for the uppermost finite volume ($n=N_{VOL}$), we have $J^n = 0$ and

$$F^n (\bar{\rho}(t + \Delta t), \bar{J}(t + \Delta t)) = \rho^n(t + \Delta t) - \rho^n(t) + \Delta t \left(d^n - q^n - \frac{J^{n-1}}{V^n} \right)_{t=t+\theta\Delta t}. \quad (\text{C.3})$$

Next, by applying the generalized midpoint rule in equation (34) to the spatially discretized conservation equation for momentum (29), the elements of

the array \bar{G} in equation (37) are found to be

$$\begin{aligned}
G^n (\bar{\rho}(t + \Delta t), \bar{J}(t + \Delta t)) = & \\
& (J^n(t + \Delta t) - J^n(t)) \left(\frac{L^n m^n(t + \theta \Delta t) + L^{n+1} m^{n+1}(t + \theta \Delta t)}{2} \right) \\
& + \Delta t \left(J^n \left(\frac{\eta^n \lambda^n L^n}{2\rho^n} + \frac{\eta^{n+1} \lambda^{n+1} L^{n+1}}{2\rho^{n+1}} \right) \right. \\
& \left. + RA_U^n (\rho^{n+1} T^{n+1} - \rho^n T^n) \right)_{t=t+\theta\Delta t}. \quad (C.4)
\end{aligned}$$

Similar to the mass conservation equation, the finite volume at the top of the fuel rod must be treated separately. For the top finite volume ($n=N_{VOL}$), the boundary condition requires the gas molar flow to be zero, which results in $G^n = 0$ for this particular volume.

We note that the change in average molar mass, m , induced by changes in the local gas composition during the time step Δt is usually very small and may in most cases be neglected. However, in equation (C.4), m is considered at the intermediate time $t = t + \theta \Delta t$.

C.2 Flow of gas constituents

As mentioned in section 4.2, residual arrays \bar{H}_i with one element per finite volume can be defined for each component i of the gas mixture. By applying the generalized midpoint rule to equation (7), the elements of \bar{H}_i can be identified as

$$\begin{aligned}
H_i^n (\bar{\rho}_i(t + \Delta t)) = & \rho_i^n(t + \Delta t) - \rho_i^n(t) \\
& + \Delta t \left(d_i^n - q_i^n + \frac{J_i^n + J_{di}^n - J_i^{n-1} - J_{di}^{n-1}}{V^n} \right)_{t=t+\theta\Delta t}, \quad (C.5)
\end{aligned}$$

where J_i , the bulk molar flow of gas component i , is calculated from equation (45) after the bulk flow of gas has been determined. The diffusive molar flow J_{di} has been determined by solving either the Stefan-Maxwell equations in (17) or the simplified equations in (19) and (21).

The lowermost and uppermost volume element in the fuel rod must be treated with special care, such that the no-flow boundary conditions are satisfied at the two ends of the flow channel. Hence, for the lowermost finite volume

($n=1$), we have $J_i^{n-1} = 0$ and

$$\begin{aligned} H_i^n(\bar{\rho}_i(t + \Delta t)) &= \rho_i^n(t + \Delta t) - \rho_i^n(t) \\ &+ \Delta t \left(d_i^n - q_i^n + \frac{J_i^n + J_{di}^n}{V^n} \right)_{t=t+\theta\Delta t}, \end{aligned} \quad (\text{C.6})$$

whereas for the uppermost finite volume ($n = N_{VOL}$), we have $J_i^n = 0$ and

$$\begin{aligned} H_i^n(\bar{\rho}_i(t + \Delta t)) &= \rho_i^n(t + \Delta t) - \rho_i^n(t) \\ &+ \Delta t \left(d_i^n - q_i^n - \frac{J_i^{n-1} + J_{di}^{n-1}}{V^n} \right)_{t=t+\theta\Delta t}. \end{aligned} \quad (\text{C.7})$$

With the residual functions defined by \bar{H}_i , a system of equations for the unknowns $\rho_i^n(t + \Delta t)$ is solved with the Newton-Raphson technique presented in section 4.1.4. Below are some remarks on the resulting system of equations and its solution in GASMIX.

Firstly, in case the diffusive molar flows in equations (C.5) to (C.7) are equal to zero, there will be no interdependence of the gas species, meaning that a linear system of equations with N_{VOL} unknowns can be solved for each gas component separately. Moreover, the Jacobian of \bar{H}_i will be the same for all the components in the gas: it will depend only on the magnitude and direction of the axial bulk flow, and on the flow channel geometry. Consequently, in absence of diffusion, the Jacobian is subjected to LR-decomposition right after it has been calculated in GASMIX. This will speed up the subsequent solutions of the linear system of equations for each gas constituent.

Secondly, if the diffusive molar flows are non-negligible, interdependence of the gas species can be avoided in the residuals \bar{H}_i and the Jacobian of \bar{H}_i , if the multicomponent diffusion is calculated with the simplified equations in (19) and (21). Hence, also in this case, a linear system of equations with N_{VOL} unknowns can be solved for each gas component separately. However, the Jacobian is not the same for all gas components in this case, so it needs to be re-calculated for each gas component.

Finally, if the diffusive molar flows are non-negligible and calculated through the Stefan-Maxwell equations, the residual functions \bar{H}_i as well the Jacobian of \bar{H}_i will exhibit interdependence of all gas components. This is due to the fact that the diffusive flux of a certain gas component, according to the Stefan-Maxwell equations, depends on the molar distribution of all the gas constituents; see equation (17). This interdependence makes it necessary to solve one large system of equations with $N_{VOL} \times N_{GAS}$ unknowns, rather than N_{GAS} similar systems with N_{VOL} unknowns in each system; N_{GAS} is here the number of gas species in the mixture. However, the solution of a large system of equations is avoided in GASMIX by introducing an "effective" diffusivity for each of the N_{GAS} constituents. More precisely, the effective diffusivity for

the i :th gas species is in GASMIX calculated through

$$D_{ie} = -j_{di} / \frac{\partial \rho_i}{\partial z}, \quad (\text{C.8})$$

where j_{di} is the diffusive molar flux, calculated either from the Stefan-Maxwell equations or the simplified equations in (19) and (21). The effective diffusivity D_{ie} represents the diffusivity that would be experienced by the i :th gas constituent, if it were in a binary gas mixture. The problem can thereby be looked upon as a simple case of binary diffusion

$$j_{di} = -D_{ie} \frac{\partial \rho_i}{\partial z}. \quad (\text{C.9})$$

When this equation is combined with the expressions for \bar{H}_i , we get N_{GAS} uncoupled systems of linear equations, each with N_{VOL} unknown molar densities of a specific gas constituent. It should be made clear that equation (C.9) is never used for calculating the diffusive flux densities j_{di} , but only when calculating the Jacobian of \bar{H}_i through equations (C.5)-(C.7). In this way, the gas components can be dealt with one at a time. The approach might be considered a bit artifact, but it is an efficient way of incorporating multi-component diffusion into the implicit time stepping scheme without having to deal with all the gas constituents simultaneously.

D GASMIX source code structure

This appendix provides a description of the numerical implementation of the GASMIX algorithm. The algorithm is implemented in FORTRAN. It is controlled from a top-level subroutine named GASMIX, from which calls are made to subordinate (lower level) subroutines and functions. In section D.1, a detailed flow chart of GASMIX is presented. Section D.2 contains a description of internal data structures that are used in the implementation.

D.1 Subroutines used in the GASMIX algorithm

A flowchart of the GASMIX algorithm with all its subordinate functions and subroutines is given in Figure D.1. The routines are used in the following context:

INPPAR: The setting of hard programmed parameters, delimiters and tolerances are gathered in this subroutine, so that they may be conveniently found and changed by the user.

INPGEO: In this subroutine, the geometrical properties of the fuel rod flow channel are set from input data. Two simple helping functions, fully described in appendix A, are used:

FLAREA: Defines the cross sectional flow area.

HAGEN: Defines the Hagen number.

INPGAS: The initial properties of the fuel rod gas inventory are found from input. The gas molar distribution, fission gas release rate, gas temperature and pressure is calculated together with the product of pressure and binary diffusion coefficients, see appendix B. Two helping functions are used:

EQSTA: The equation of gas state.

PBDC: Calculates product of gas pressure and the binary diffusion coefficients D_{ik} .

GLEAK: Subroutine used for calculating the current rate of outflow or inflow to a leaking segment of the fuel rod. Only outleakage is supported in the present program version.

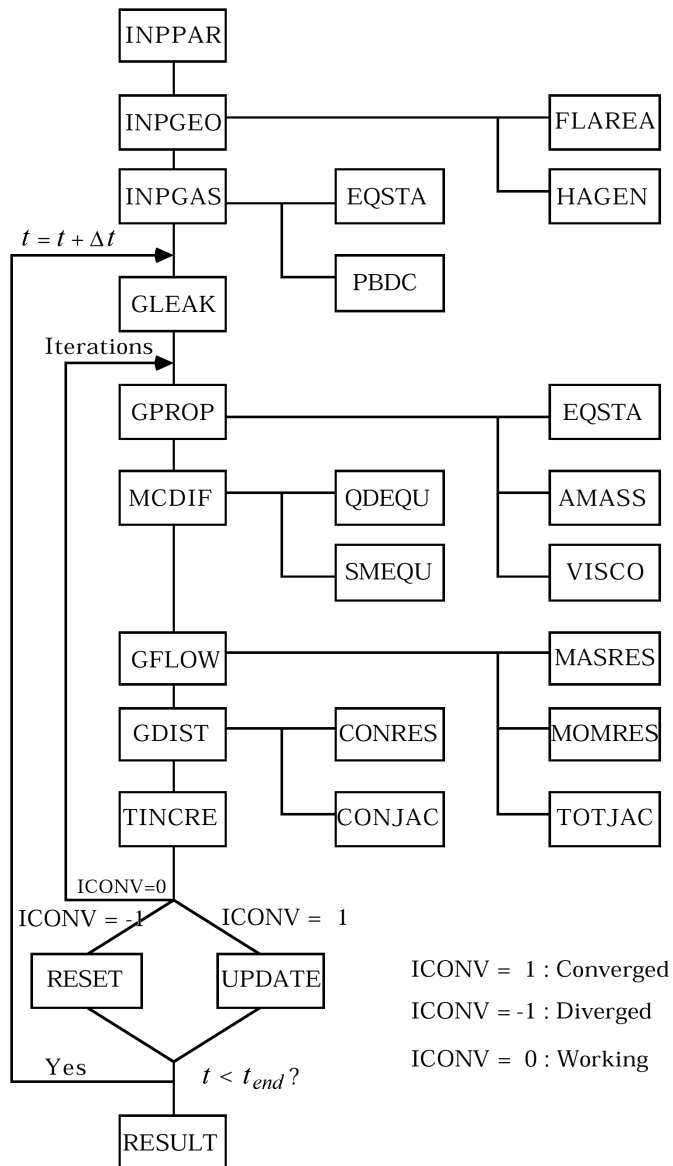


Figure D.1: Flowchart of the GASMIX subroutine with calls to all subordinate procedures and functions.

GPROP: Subroutine calculates the current gas properties; pressure, molar composition, average molar mass and dynamic viscosity. Three helping functions are used:

EQSTA: The equation of gas state.

AMASS: Calculates molar mass.

VISCO: Calculates gas dynamic viscosity.

MCDIF: Subroutine solves the equations of multi-component diffusion. Output consists of the diffusive molar fluxes at the finite volume interfaces. Two different methods can be chosen by the user in order to calculate these fluxes:

QDEQU: The simplified equations for binary diffusion in a matrix of helium are used.

SMEQU: The Stefan-Maxwell equations for multi-component diffusion are used.

GFLOW: The axial bulk molar flow is calculated by simultaneously solving the equations of mass and momentum. This is done by first calculating the equation system residuals and Jacobian matrix, and then solving the linearized system of equations:

MASRES: Calculates residuals from unbalance in the bulk mass conservation equation.

MOMRES: Calculates residuals from unbalance in the momentum conservation equation.

TOTJAC: Calculates the total Jacobian of the mass and momentum equations.

GDIST: Calculates the change in molar distribution due to bulk flow and diffusion. The change in gas distribution with respect to individual constituents is calculated by solving the component form of the continuity equation:

CONRES: Calculates residuals from unbalance in the mass equation for each constituent.

CONJAC: Calculates the Jacobian of the mass conservation equation for each constituent.

TINCRC: Subroutine controls the iteration procedure and sets a new micro-scale timestep, the length of which is determined by the rate of convergence in the inner iterations. Depending on the magnitude of the residuals calculated in the last step of GDIST, a status variable ICONV is set to either of the following values:

ICONV = 1: Iterations have converged; residuals are below the preset tolerance.

ICONV = -1: Iterations are diverging; increasing residuals have been detected.

ICONV = 0: Iterations have not yet converged, but the residuals are decreasing.

UPDATE: Subroutine called in case $ICONV = 1$. Molar distribution, gas bulk velocity and current time is updated before passing to a new micro-scale timestep.

RESET: Subroutine called in case $ICONV = -1$. The initial trial guess on the molar distribution at the end of the timestep is reset, and new iterations are initiated, utilizing a shorter micro-scale timestep.

RESULT: Transfer the calculated results regarding the gas molar distribution and pressure to the global data arrays of the host code.

D.2 Data structures used in GASMIX

In the following section, internal data arrays used in the GASMIX subroutine are listed with respect to size and contents. The size of these arrays is characterized by the following delimiters:

NVOL Number of finite volumes (axial segment) along the fuel rod

NGAS Number of gas components treated by GASMIX

D.2.1 Flow channel data

GTVOL(NVOL) Total gas volume in the finite volume [m^3]

GSCSA(NVOL) Axial segment cross sectional area [m²]

GSHYD(NVOL) Segment hydraulic diameter [m]

GSFRF(NVOL) Geometrical flow resistance factor[m⁻²]

GSHAG(NVOL) Axial segment Hagen number [-]

GSAXL(NVOL) Axial segment length [m]

D.2.2 Gas inventory data

GTMOL(NVOL) Total (bulk) gas inventory in finite volumes [mol]

GPMOL(NVOL,NGAS) Partial gas inventory in finite volumes [mol]

GTFGR(NVOL) Total (bulk) fission gas release rate [mols⁻¹]

GPFGR(NVOL,NGAS) Partial fission gas release rate [mols⁻¹]

GPFRA(NVOL,NGAS) Molar fractions of the gas mixture [-]

GTMMA(NVOL) Total molar mass for the gas [kgmol⁻¹]

GCAVE(NGAS) Rod average molar composition (in fractions) [-]

D.2.3 Gas thermodynamic data

GTMOD(NVOL,2) Total gas molar density (old/new) [molm³]

GPMOD(NVOL,NGAS,2) Partial gas molar density (old/new) [molm³]

GTEMP(NVOL) Temperature of the mobile part of the gas [°C]

GTPRS(NVOL) Gas total pressure in finite volumes [Pa]

GTVTF(NVOL) V/T-fraction of the total gas volume [m³K⁻¹]

GTVSC(NVOL) Gas dynamic viscosity [Nsm⁻²]

GPBDC(NVOL,NGAS,NGAS) Pressure times binary diffusivities [Ns⁻¹]

EDIFC(NVOL,NGAS) Effective binary diffusivities in helium [m²s⁻¹]

D.2.4 Gas transport data

BFLOW(NVOL,2) Gas bulk molar flow (old/new) [mols⁻¹]

DFLOW(NVOL,NGAS) Gas diffusive molar flow [mols⁻¹]

GTOUT(NVOL) Gas total (bulk) outflow rate [mols⁻¹]

GPOUT(NVOL,NGAS) Gas partial (component) outflow rate [mols⁻¹]

D.2.5 Work arrays for equation solvers

GMAT1(NVOL*2,NVOL*2) System matrix for bulk flow solution [-]

GARR1(NVOL*2) Load array for bulk flow solution [-]

IARR1(NVOL*2) Pivot index array for bulk flow solution [-]

GMAT2(NVOL,NVOL) System matrix for component flow solution [-]

GARR2(NVOL) Load array for component flow solution [-]

IARR2(NVOL) Pivot index array for component flow solution [-]

GMAT3(NGAS,NGAS) System matrix for diffusive flow solution [-]

GARR3(NGAS) Load array for diffusive flow solution [-]

IARR3(NGAS) Pivot index array for diffusive flow solution [-]



2020:02

The Swedish Radiation Safety Authority has a comprehensive responsibility to ensure that society is safe from the effects of radiation. The Authority works to achieve radiation safety in a number of areas: nuclear power, medical care as well as commercial products and services. The Authority also works to achieve protection from natural radiation and to increase the level of radiation safety internationally.

The Swedish Radiation Safety Authority works proactively and preventively to protect people and the environment from the harmful effects of radiation, now and in the future. The Authority issues regulations and supervises compliance, while also supporting research, providing training and information, and issuing advice. Often, activities involving radiation require licences issued by the Authority. The Swedish Radiation Safety Authority maintains emergency preparedness around the clock with the aim of limiting the aftermath of radiation accidents and the unintentional spreading of radioactive substances. The Authority participates in international co-operation in order to promote radiation safety and finances projects aiming to raise the level of radiation safety in certain Eastern European countries.

The Authority reports to the Ministry of the Environment and has around 300 employees with competencies in the fields of engineering, natural and behavioural sciences, law, economics and communications. We have received quality, environmental and working environment certification.

Strålsäkerhetsmyndigheten
Swedish Radiation Safety Authority

SE-17116 Stockholm

Tel: +46 8 799 40 00

E-mail: registrator@ssm.se

Web: stralsakerhetsmyndigheten.se